

Radiation of Neutron Stars Produced by Superfluid Core

Anatoly A. Svidzinsky

Bartol Research Institute, University of Delaware, Newark, DE 19716, USA
asvid@bartol.udel.edu

ABSTRACT

We find a new mechanism of neutron star radiation wherein radiation is produced by the stellar interior. The main finding is that neutron star interior is transparent for collisionless electron sound, the same way as it is transparent for neutrinos. In the presence of magnetic field the electron sound is coupled with electromagnetic radiation, such collective excitation is known as a fast magnetosonic wave. At high densities the wave reduces to the zero sound in electron liquid, while near the stellar surface it is similar to electromagnetic wave in a medium. We find that zero sound is generated by superfluid vortices in the stellar core. Thermally excited helical vortex waves produce fast magnetosonic waves in the stellar crust which propagate toward the surface and transform into outgoing electromagnetic radiation. The magnetosonic waves are partially absorbed in a thin layer below the surface. The absorption is highly anisotropic, it is smaller for waves propagating closer to the magnetic field direction. As a result, the vortex radiation is pulsed with the period of star rotation. The vortex radiation has the spectral index $\alpha \approx -0.45$ and can explain nonthermal radiation of middle-aged pulsars observed in the infrared, optical and hard X-ray bands. The radiation is produced in the star interior, rather than in magnetosphere, which allows direct determination of the core temperature. Comparing the theory with available spectra observations we find that the core temperature of the Vela pulsar is $T \approx 8 \times 10^8 \text{K}$, while the core temperature of PSR B0656+14 and Geminga exceeds $2 \times 10^8 \text{K}$. This is the first measurement of the temperature of a neutron star core. The temperature estimate rules out equation of states incorporating Bose condensations of pions or kaons and quark matter in these objects. The estimate also allows us to determine the critical temperature of triplet neutron superfluidity in the Vela core $T_c = (7.5 \pm 1.5) \times 10^9 \text{K}$ which agrees well with recent data on behavior of nucleon interactions at high energies. We also find that in the middle aged neutron stars the vortex radiation, rather than thermal conductivity, is the main mechanism of heat transfer from the stellar core to the surface. The core radiation opens a possibility to study composition of neutron star crust by detection absorption lines corresponding to the low energy excitations of crust nuclei. Bottom layers of the crust may contain exotic nuclei with the mass number up to 600 and the core radiation creates a perspective to study their properties. In principle, zero sound can also be emitted by other mechanisms, rather than vortices. In this case the spectrum of stellar radiation would contain features corresponding to such processes. As a result, zero sound opens a perspective of direct spectroscopic study of superdense matter in the neutron star interiors.

1. Introduction

Properties of matter at densities much larger than nuclear are poorly known and constitute a challenging problem of modern science. They have broad implications of great importance for cosmology, the early

universe, its evolution, for compact stars and for laboratory physics of high-energy nuclear collisions. Present searches of matter properties at high density take place in several arenas. One of them is investigation of neutron stars.

According to theory of neutron stars (NSs) (Yakovlev et al. 1999a) a NS can be subdivided into the atmosphere and four internal regions: the outer crust, the inner crust, the outer core and the inner core as shown in Fig. 1. The atmosphere is a thin plasma layer, where thermal electromagnetic radiation is formed. The depth of the atmosphere varies from some ten centimeters in a hot NS down to some millimeters in a cold one. The outer crust extends from the bottom of the atmosphere to the layer of density $\approx 4.3 \times 10^{11} \text{g/cm}^3$ and has a depth of several hundred meters. Ions and electrons compose its matter. The depth of the inner crust may be as large as several kilometers. The inner crust consists of electrons, free neutrons and neutron-rich atomic nuclei. Neutrons in the inner crust are in a superfluid state. The outer core occupies the density range $0.86 - 2\psi_0$, where $\psi_0 = 2.8 \times 10^{14} \text{g/cm}^3$ is the saturation nuclear matter density, and can be several kilometers in depth. It consists of neutrons n with some (several per cent by particle number) admixture of protons p and electrons e . Almost all theories of NSs predict the appearance of neutron superfluidity and proton superconductivity in the outer NS core. In a low-mass NS, the outer core extends to the stellar center.

More dense NSs also possess an inner core (see Fig. 1). Its radius may reach several kilometers and central density may be as high as $10 - 15\psi_0$. The composition and equation of state of the inner core are poorly known and it constitutes the main NS “mystery”. Several hypotheses are discussed in the literature. One of them is appearance of Σ - and Λ -hyperons in the inner core. The second hypothesis assumes the appearance of pion condensation. The third hypothesis predicts a phase transition to strange quark matter composed of almost free u , d and s quarks with a small admixture of electrons. Several authors also considered the hypothesis of kaon condensation in the dense matter. The radius of the NS usually decreases as the stellar mass increases (NS becomes more compact). The mass reaches its maximum at some density, which corresponds to the most compact stable stellar configuration. Typically the stellar mass ranges between $0.5 - 3M_\odot$ for different equations of state (M_\odot is the solar mass).

Despite of 30 years enormous theoretical and observational efforts, the properties of matter in neutron star cores remain poorly known. The main reason is that detected thermal radiation from the star surface carries practically no information about the stellar interior. Some indirect methods, such as estimates of neutron star masses, radii and cooling rates for different equation of states, have been applied to find constrains on the matter behavior. However, non of them is reliable enough because the answer strongly depends on the model parameters which are also poorly known.

In this paper we discuss a new direct way to determine properties of the superdense matter. We found that neutron star interior is transparent for electron zero sound, the same way as it is transparent for neutrinos. Zero sound is a collective density (or spin-density) wave in Fermi liquids that was predicted by Landau in 1957 and later observed in ^3He and electron liquid in metals. The wave frequency ω is greater then the frequency of interparticle collisions which makes the wave different from usual hydrodynamic sound. In neutron stars the zero sound can propagate in electron fluid which fills the stellar crust and core, the collisionless (zero sound) regime is reached at $\omega/2\pi > 10^{12} \text{Hz}$. The large density of electrons in NS interior results in substantial reduction of the interaction energy between fermions as compared to their kinetic (Fermi) energy, the electron gas becomes more ideal. In such weakly interacting Fermi system the attenuation of zero sound is exponentially small (see Eq. (A9) in Appendix A). As a result, zero sound propagates across the star in a ballistic regime, which is similar to neutrino. However, this is not the case for single-particle excitations in electron liquid, their mean free path usually does not exceed $0.01 - 1 \text{cm}$. The single-particle

excitations are in a local thermodynamic equilibrium with the stellar matter, while collective zero sound modes do not. At the same time, negligible attenuation of the zero sound creates an obstacle to excite such waves inside the stellar medium. Some special processes are required for their generation. We found that zero sound is generated at the core-crust interface by helical motion of superfluid vortices. Vortex modes themselves are excited thermally via single-particle channel, they are in thermodynamic equilibrium with the surrounding medium.

In the presence of magnetic field the electron sound is coupled with electromagnetic radiation, such excitation is known as a fast magnetosonic wave. At large densities the effect of magnetic field is negligible and the wave behaves as a sound wave, however near the stellar surface (small matter density) it reduces to electromagnetic wave which leave the star and propagates into surrounding space. Such property results in a new mechanism of star radiation produced at the stellar interior. Contrary to neutrino, electromagnetic radiation is easy to detect which opens a perspective of direct spectroscopic study of superdense matter. Thermally excited helical vortex waves generate fast magnetosonic waves in the stellar crust which propagate toward the surface and transform into outgoing electromagnetic radiation. We found that such mechanism results in radiation with non Planck's spectrum (Eqs. (23), (42)) and theoretical predictions agree well with nonthermal radiation of some middle-aged pulsars observed in the infrared, optical and hard X -ray bands (Figs. 5, 6). The important result of our theory is that detection of vortex radiation in the X -ray band allows direct determination of the core temperature. From available spectral data we found that the core temperature of the Vela pulsar is $T \approx 8 \times 10^8 \text{K}$, while the core temperature of PSR B0656+14 and Geminga exceeds $2 \times 10^8 \text{K}$. This is the first measurement of the temperature of a NS core. The cooling rate and temperature of the central part of a NS substantially depends on the properties of dense matter. Our temperature estimate excludes exotic equation of states incorporating Bose condensations of pions or kaons and quark matter in these objects. Such conclusion agrees with recent measurement of gravitational redshift of a neutron star (Cottam et al. 2002). Moreover, the temperature estimate allows us to determine the temperature of superfluid transition of neutrons in the Vela core $T_c = (7.5 \pm 1.5) \times 10^9 \text{K}$. This value agrees well with theoretical predictions that are based on new nucleon-nucleon interaction potentials which fit the recent world data for pp and np scattering up to 500Mev (Baldo et al. 1998; Arndt et al. 1997). Examples of such potentials are Nijmegen I and II. For the matter density $2\psi_0$ (which is a central region density of a canonical NS without exotic inner core) these nucleon potentials predict $T_c \approx 7.5 \times 10^9 \text{K}$ for neutron superfluidity with 3P_2 (triplet) pairing (Baldo et al. 1998). One should mention that in order to find the transition temperature at densities up to $10\psi_0$ more accurate potentials which fit the measured nucleon-nucleon phase shifts up to about 1Gev are required. A systematic study of pulsar radiation in the X -ray band can locate objects with fast cooling core which could be candidates for NSs with exotic states of matter.

The plan of the paper is the following. In section 2 we discuss neutron vortices in the superfluid core and generation of magnetosonic waves by vortices at the crust-core interface. In sections 3, 4 we investigate propagation of magnetosonic waves across the stellar crust and their transformation into electromagnetic radiation at the surface. In section 5 we consider spectrum of electromagnetic radiation produced by vortices and analyze the applicability of our results. In section 6 we compare the theory with radiation spectrum of some middle-aged pulsars observed in infrared- X -ray bands and discuss properties of superdense matter based on the observed spectra. Section 7 is devoted to a problem of heat transport across the stellar crust. In section 8 we draw our conclusions and discuss perspectives in the field. In Appendices A, B, C we consider zero sound in an electron liquid, derive equations of collisionless magnetic hydrodynamics for electron motion in the stellar crust and investigate propagation of electromagnetic waves across the atmosphere.

2. Vortex radiation in rotating neutron stars

If a NS rotates with an angular velocity $\boldsymbol{\Omega} = \Omega \hat{z}$ a periodic vortex lattice forms in a superfluid neutron phase of the stellar core. Typical value of the lower critical angular velocity of the vortex formation is $\Omega_{c1}/2\pi \sim 10^{-14} \text{s}^{-1}$ (Sedrakyan & Shakhabyan 1991). The vortices are parallel to the axis of rotation apart from a tiny region ($\leq 10^{-3} \text{cm}$) near the condensate surface, where they are curved and cross the boundary in the perpendicular direction. The distance between vortices in a triangular lattice is $b = (4\pi\hbar/\sqrt{3}M\Omega)^{1/2}$, where M is the mass of the condensate particles. E.g., for a neutron superfluid ($M = 2m_n$, where m_n is the neutron mass) and $\Omega/2\pi = 10 \text{s}^{-1}$ the lattice period $b = 6 \times 10^{-3} \text{cm}$. For NSs the characteristic size of the vortex core is $\xi = 10^{-12} \text{cm}$, so that $b \sim 10^{10}\xi$ and the total number of vortices in the superfluid $N = MR^2\Omega/\hbar \approx 10^{17}$, where $R \approx 10 \text{km}$ is the radius of the superfluid condensate (Sedrakyan & Shakhabyan 1991).

First, let us consider a single straight vortex line with length L located in a spherical one component superfluid condensate. We assume the condensate density is uniform inside the sphere. One should note that this situation differs from real NS core which consists of a mixture of neutrons, protons and electrons. However, main properties of vortices can be understood within the simplified model. Normal modes of the vortex are helical waves (Lifshitz & Pitaevskii 1980)

$$r = A \exp(i\omega t + ik_{\parallel} z), \quad \omega = \frac{\hbar}{2M} k_{\parallel}^2 \ln(1/k_{\parallel}\xi), \quad (1)$$

where A is the amplitude and k_{\parallel} is the wave number. Eqs. (1) are valid for $k_{\parallel}\xi \ll 1$, or $\omega \ll \omega_c = \hbar/2M\xi^2 \approx 10^{20} \text{Hz}$ and describe rotation of a helix with the angular frequency ω .

To find the amplitude of the helical waves A one can use the expression for the energy of the system in terms of normal vortex modes (Svidzinsky & Fetter 2000a). If a superfluid contains a vortex line of length L it changes the kinetic energy of the fluid by

$$E_k = \int \frac{MnV^2}{2} d^3r = \pi Ln \frac{\hbar^2}{M} \ln(b/\xi), \quad (2)$$

where n is the superfluid particle density. Change in the kinetic energy (2) gives the main contribution to the change in the fluid energy. One should mention that the superfluid density is suppressed near the vortex core. However, the normal component fills the vortex core so that the total fluid density remains approximately constant (Nygaard et al. 2002). This occurs because any variation in the total density in a Fermi liquid (under NS conditions) produces substantial change of the Fermi energy and increases the energy of the system. The same situation takes place during the vortex motion and, as a result, the helical vortex waves are not accompanied by oscillation in the total density. In the wave the superfluid and normal components oscillate in the opposite phase so that the total fluid density remains approximately constant.

Taking into account that excitation of the helical wave (1) changes the vortex length by the value $LA^2k_{\parallel}^2/2$, one can obtain the energy of the system in terms of normal mode amplitudes (Svidzinsky & Fetter 2000a)

$$E = E_0 + \pi nL \sum_m A_m^2 \hbar \omega_m. \quad (3)$$

In the NS core the helical vortex waves are excited thermally by particle scattering on the vortex cores. Vortex excitations are in a local thermal equilibrium with the stellar matter. Then at temperature T the

energy of the wave with the frequency ω is equal to $\hbar\omega$ times the mean number $1/[\exp(\hbar\omega/k_B T) - 1]$ of excitations in that state. Therefore, the vortex wave amplitude is given by (cf. (Barenghi 1996))

$$A^2 = \frac{1}{\pi n L [\exp(\hbar\omega/k_B T) - 1]}, \quad (4)$$

where k_B is Boltzmann's constant. For typical parameters of NSs $A \ll \xi$. Indeed, if we take $n = 10^{39} \text{cm}^{-3}$, $L = 10 \text{km}$, $\omega/2\pi = 10^{15} \text{Hz}$, $T = 10^8 \text{K}$ and $\xi = 10^{-12} \text{cm}$, we obtain for the amplitude of the thermally excited helical wave $A \approx 10^{-9} \xi$.

Apart from helical waves there are excitations of the vortex lattice in a plane perpendicular to the vortex lines which correspond to relative displacements of vortices with respect to each other (the so called Tkachenko's modes). These excitations are analogous to a vortex precession in trapped Bose-Einstein condensates where a vortex line moves along a trajectory with constant trapping potential (Svidzinsky & Fetter 2000b). However, frequencies of the vortex oscillation due to excitation of such modes are small. Indeed, the frequency of Tkachenko's modes is given by $\omega_T = \sqrt{\hbar\Omega/4M} k_\perp$, where k_\perp is the wavenumber in the plane perpendicular to vortices (Tkachenko 1965). For maximum frequency $k_\perp \sim 1/b$, where b is the lattice spacing, and we obtain $\omega_{T \text{ max}} \sim \Omega$, which is much less than frequencies of radiation we are interested in.

2.1. Energy transport by helical vortex waves in superfluids

Let us consider a superfluid with a vortex line located along the z axis and introduce perturbation in the particle density n' and the velocity potential χ' : $n = n_0 + n'$, $\chi = \chi_0 + \chi'$, where $n_0 = n_0(\mathbf{r})$ is the superfluid density for a straight vortex line and $\chi_0 = \hbar\phi/M$. At distances $r \lesssim \xi$ (we use cylindrical coordinates r, ϕ, z measured from the center of the vortex line) the helical vortex motion (1) can be described in terms of n' and χ' as

$$n' = -A \exp [i(\omega t + k_\parallel z - \phi)] \frac{\partial n_0}{\partial r}, \quad (5)$$

$$\chi' = iA \frac{\hbar}{Mr} \exp [i(\omega t + k_\parallel z - \phi)]. \quad (6)$$

In the bulk the function χ' (as well as n') should satisfy a linearized equation of superfluid hydrodynamics, which is, in fact, the wave equation for sound propagation

$$\frac{\partial^2 \chi'}{\partial t^2} - c_s^2 \nabla^2 \chi' = 0, \quad (7)$$

where c_s is the speed of sound in superfluid. In the limit $\omega \ll \omega_c$ one can omit the first term in Eq. (7). Then solution of this equation which satisfies the boundary condition (6) has the form

$$\chi' = iA \frac{\hbar k_\parallel}{M} K_1(k_\parallel r) \exp [i(\omega t + k_\parallel z - \phi)], \quad (8)$$

where K_1 is the modified Bessel function. The solution exponentially decreases at $r \gg 1/k_\parallel$: $K_1(k_\parallel r) \approx (\pi/2k_\parallel r)^{1/2} \exp(-k_\parallel r)$. We obtain that helical vortex waves produce perturbation in the superfluid velocity $\mathbf{V} = \nabla\chi$ which is localized near the vortex core. Such perturbation results in the energy flow along the vortex line so that the energy flux is localized near the vortex.

The energy flux can be estimated as

$$\mathbf{Q} = \int \frac{1}{2} \rho V'^2 \frac{\partial \omega}{\partial \mathbf{k}} dS, \quad (9)$$

where $\rho = Mn$ is the superfluid density, V' is the perturbation in the superfluid velocity due to helical vortex motion and $\partial\omega/\partial\mathbf{k} = \hbar k_{\parallel} \ln(1/k_{\parallel}\xi)\hat{z}/M$ is the group velocity of the helical wave. In Eq. (9) the integral is taken in a plane perpendicular to the vortex line. Then, we note that $L \int \frac{1}{2}\rho V'^2 dS$ is the total energy of the helical wave, which at temperature T is given by

$$L \int \frac{1}{2}\rho V'^2 dS = \frac{\hbar\omega}{\exp(\hbar\omega/k_B T) - 1}. \quad (10)$$

Taking Eq. (10) into account, we find the following expression for the energy flux along the vortex:

$$Q = \frac{\hbar^{3/2}\omega^{3/2}\sqrt{\ln(\omega_c/\omega)}}{L\sqrt{M}[\exp(\hbar\omega/k_B T) - 1]}. \quad (11)$$

The number of vortex modes within the interval dk_{\parallel} is $Ldk_{\parallel}/2\pi = L\sqrt{M}d\omega/2\pi\sqrt{\hbar\omega \ln(\omega_c/\omega)}$ and, hence, the spectral power density of energy flux along a single vortex line is

$$P(\omega) = \frac{\hbar\omega}{2\pi[\exp(\hbar\omega/k_B T) - 1]}. \quad (12)$$

This expression is a universal function in the sense that it depends only on the temperature. At $\hbar\omega < k_B T$ the energy spectrum is independent of frequency and $P = k_B T/2\pi$.

One should note that the energy flow produced by helical waves substantially differs from energy radiation in the case of a moving straight vortex line. A moving straight vortex in a compressible fluid emits sound waves in the direction perpendicular to the vortex line. A homogeneous two-dimensional (2D) superfluid is equivalent to (2+1)-dimensional electrodynamics, with vortices playing the role of charges and sound corresponding to electromagnetic radiation (Ambegaokar et al. 1980; Arovas & Freire 1997; Ovchinnikov & Sigal 1998; Fischer 1999; Lundh & Ao 2000). Thus, radiation of sound waves from a straight vortex moving on a circular trajectory is concentrated in a plane perpendicular to the vortex line and can be estimated using formulas for the cyclotron radiation of an electrical charge moving along a circular orbit in 2D space.

To understand the difference between energy radiation by a straight vortex and a helical wave we can solve the problem in general case. Indeed, general solution of Eq. (7) that satisfies the asymptotic behavior (6) is

$$\chi' = -\frac{i\pi\hbar A}{2M}k_{\perp}Y_1(k_{\perp}r)\exp[i(\omega t + k_{\parallel}z - \phi)], \quad (13)$$

where Y_1 is the Bessel function and $k_{\perp} = \sqrt{\omega^2/c_s^2 - k_{\parallel}^2}$. At large r the solution (13) has the asymptotic

$$\chi' = -\frac{i\sqrt{\pi}\hbar A\sqrt{k_{\perp}}}{\sqrt{2M}\sqrt{r}}\sin\left(k_{\perp}r - \frac{3\pi}{4}\right)\exp[i(\omega t + k_{\parallel}z - \phi)], \quad (14)$$

$$n' = -\frac{n}{c_s^2}\frac{\partial\chi'}{\partial t} = -\frac{\sqrt{\pi}\hbar\omega n A}{\sqrt{2M}c_s^2\sqrt{r}}\sqrt{k_{\perp}}\sin\left(k_{\perp}r - \frac{3\pi}{4}\right)\exp[i(\omega t + k_{\parallel}z - \phi)]. \quad (15)$$

For $\omega > c_s k_{\parallel}$ (k_{\perp} is a real number) the solution describes radiation of sound waves with a conical wavefront (the cone angle is $\arctan(k_{\perp}/k_{\parallel})$). The particular case $k_{\parallel} = 0$ corresponds to a circular motion of a straight vortex and sound waves are radiated in the plane perpendicular to the vortex line. However, in the case of helical waves the wavelength of sound that would be emitted is much larger than the wavelength of helical wave and the condition of sound radiation $\omega > c_s k_{\parallel}$ (which for a helix is equivalent to $\omega > 4\omega_c/\ln(\omega_c/\omega)$) fails. As a result, the solution (13) reduces to (8) which describes energy flow along the vortex.

2.2. Magnetic field associated with neutron vortices

Now let us take into account a superconducting proton component in NS core. The bulk of superconducting protons do not rotate by forming vortices, which differs from neutron superfluid. Superconducting protons corotate with the crust and electron fluid by generating a surface current which produces a small uniform magnetic field in the interior $\mathbf{H} = -2m_p c \boldsymbol{\Omega} / e$, here m_p , e is the proton mass and charge (Alpar et al. 1984). The vector potential associated with this field $\mathbf{A} = -m_p c (\boldsymbol{\Omega} \times \mathbf{r}) / e$ yields the proton velocity which corresponds to rigid body rotation

$$\mathbf{V}_p = \frac{\hbar}{2m_p} \left(\nabla\varphi - \frac{2e}{\hbar c} \mathbf{A} \right) = \boldsymbol{\Omega} \times \mathbf{r},$$

while the phase of the proton order parameter φ is constant inside the superconductor. However, due to interactions between protons and neutrons, neutron superfluid velocity generates a superfluid current of protons in the vicinity of neutron vortices (drag effect) and an associated magnetic field around each neutron vortex line. The magnetic field of a neutron vortex is confined within a radius of the order of the effective London length $\Lambda_*^2 = m_p m_p^* c^2 / 4\pi e^2 \rho_p$, where ρ_p is the mass density of superfluid protons and m_p^* is the proton effective mass (Alpar et al. 1984). For the interior density $\rho_n = 10^{14} \text{g/cm}^3$ and proton concentration $\rho_p / \rho_n = 0.05$ the screening length is $\Lambda_* \approx 10^{-11} \text{cm}$. At $r \geq \xi$ the magnetic field is given by

$$\mathbf{H}_v = \frac{\Phi_* K_0(r/\Lambda_*)}{2\pi \Lambda_*^2} \hat{z}, \quad (16)$$

where $\Phi_* = \Phi_0 \delta m_p^* / m_n$, $\Phi_0 = \pi \hbar c / e$ is the flux quantum, $\delta m_p^* = m_p^* - m_p$ is the contribution to the proton effective mass due to the interaction with the neutron medium and K_0 is the modified Bessel function. Sjöberg (1976) has shown that for typical barion densities of a NS core $1 - 6 \times 10^{14} \text{g/cm}^3$ the ratio m_p^* / m_p changes approximately from 0.5 to 0.25. This result is important for our theory since it indicates that neutron vortices are strongly coupled with protons that carry electric charge. As a consequence, motion of neutron vortices is accompanied by motion of protons and, therefore, electrons. This creates a possibility of excitation collective modes in the electron liquid by oscillating neutron vortices. In superconducting (npe) phase the magnetic field lines are parallel to neutron vortices which is similar to magnetic field of a long solenoid with the radius Λ_* . In the stellar crust there is no drag effect and magnetic lines diverge the same way as magnetic lines near the edge of the solenoid.

One should note that fossil (not associated with neutron vortices) magnetic field can exist in the stellar core. However, the process of the magnetic fields generation in NSs and, hence, their structure and localization is still under discussion. There are arguments that NS magnetic fields may be confined to the crustal layer only, where it has been generated by thermomagnetic instability during the first years of NS evolution (Blandford et al. 1983; Urpin et al. 1986; Wiebicke & Geppert 1996). However, there is a possibility that magnetic field permeates both the stellar crust and the core. Such magnetic field (if it exists) forms before the transition into superconductivity by convection which arises in first 10-20 seconds after the NS is born and most probably, has a very complicated twisted structure (Thompson & Duncan 1993). As a rule the magnetic flux tubes inside a neutron star do not parallel to the axis of rotation (Ruderman et al. 1998). One should mention, that typical value of the critical field for vortex formation in superconducting core, 10^{15}Gs , is much greater than actual magnetic field in NSs 10^{12}Gs . Therefore, the core state with penetrating fossil magnetic field is metastable. Proton vortices are expelled from superconductor by different dissipation mechanisms which determine the life time of the metastable configuration. One of the mechanisms is the following. Since the neutron vortex and a flux tube strongly interact as they pass through each other, the

moving neutron vortices will push on the proton’s flux-tube array, forcing it to move outside in a spinning-down NS (Sauls 1989). As neutron vortex motion moves an entrained flux tube, that tube is ultimately pushed into the crust-core interface for almost any initial flux-tube configuration. E.g., during the spinning-down stage when the initial stellar rotation period of 1ms (at the star birth) increases to 100ms (middle aged pulsars) the spacing between neutron vortices increases by a factor of 10. As a result all magnetic tubes should be pushed out into the crust unless originally some of them pass very close (at a distance less than 0.1 stellar radii) to the axis of rotation.

In this paper we will not consider possible presence of fossil magnetic tubes in the stellar core. Such tubes would not modify radiation produced by neutron vortices, however, they may give an additional contribution into stellar radiation. The main reason why we do not consider the possible presence of fossil magnetic tubes is that the observed spectra of middle aged pulsars can be explained well only by radiation from neutron vortices. The other argument is that the core temperature we determined from the observed spectra is very high. The big difference between the core and surface temperatures suggests strong heat isolation of the stellar core. In Sec. 7 we show that geometry in which magnetic lines at the crust bottom are parallel to the core surface (or magnetic field has a closed configuration within the star) provides sufficient heat isolation and can explain the observations. Such geometry suggests that fossil magnetic field, if it has been generated in the core, already expelled from the superconducting core at the stage of middle aged pulsars. Based on the results of this paper we can provide another argument against presence of fossil magnetic field in the stellar core. The point is that our findings show that superfluidity of neutrons and superconductivity of protons in the NS core are very strong. Such conclusion is also supported by the theory which is based on new realistic interaction potentials between nucleons (Baldo et al. 1998; Elgaroy et al. 1996). The temperature of superconducting transition for protons near the stellar center is expected to be no less than $2 \times 10^{10}\text{K}$ (Elgaroy et al. 1996). The modified Urca process cools the stellar core to such temperature during the time $\tau \approx 1\text{yr}/T_9^6 = 0.5\text{s}$ (Pethick 1992). This means that stellar interior practically instantly after the star formation becomes superconducting and the convection mechanism cannot generate magnetic field at the stellar core simply because there is no time for that.

2.3. Generation of magnetosonic waves at the boundary of superconducting phase

At the interface between the stellar crust and the outer core (at the density $2.4 \times 10^{14}\text{g}/\text{cm}^3$) the matter undergoes a first order transition from a nucleus-electron-neutron (*Aen*) phase to a uniform liquid of neutrons, protons and electrons (*npe* phase). Nuclei in the *Aen* phase can be spherical and form a Coulomb crystal or have a deformed shape which results in an exotic distributions of nuclear matter. Transition from the *Aen* phase to the uniform liquid is accompanied by a small (about 1.4%) density jump (Douchin & Haensel 2000). In the *npe* phase the proton liquid is superconducting (Baym et al. 1969), while in the *Aen* phase protons constitute a part of nuclei. As a result, the *Aen* phase is not superconducting, however, neutron component is still superfluid.

As we have shown before, helical vortex motion does not generate sound waves in the stellar core because the condition of sound radiation is not satisfied. However, at the interface between the superconducting (*npe*) and *Aen* phases such vortex motion produces magnetosonic waves which propagate across the stellar crust toward the surface. One should note that frequencies of radiation we are interested in are larger than effective frequencies of electron-phonon and electron-electron collisions $\nu_{e,\text{ph}}$, $\nu_{e,e}$. According to Eqs. (30), (45) at $T = 10^8\text{K}$, $\rho = 10^{14}\text{g}/\text{cm}^3$, $n_e = 10^{37}\text{cm}^{-3}$ for ^{56}Fe lattice we obtain $\nu_{e,\text{ph}} = 8 \times 10^{11}\text{s}^{-1}$, $\nu_{e,e} = 10^{10}\text{s}^{-1}$. So, at $\omega/2\pi > 10^{12}\text{Hz}$ the electrons in the stellar crust behave as an independent system of Fermi particles and

move in collisionless regime. In such regime a zero sound is a possible collective excitation of Fermi liquid. In details the zero sound in electron liquid is discussed in Appendix A. In the presence of magnetic field the electron sound is coupled with electromagnetic radiation. In Appendix B we derive equations of electron motion in collisionless regime and show that they reduce to usual equations of magnetic hydrodynamics in which speed of zero sound enters the equations instead of speed of usual sound and the Alfvén velocity is estimated in terms of the electron density $\rho_e = m_e n_e$: $u_A = H/\sqrt{4\pi\rho_e}$. One should mention that near the crust bottom the Alfvén velocity is small because of large density. If $H = 10^{12}\text{Gs}$ and $\rho_e = 10^{11}\text{g/cm}^3$ we obtain $u_A = 9 \times 10^5\text{cm/s}$ which is much less than the speed of zero sound $u_s \approx c$, where c is the speed of light. In magnetic hydrodynamics there are three possible types of waves: Alfvén, fast and slow magnetosonic. Here we consider radiation of fast magnetosonic waves which are in the limit $u_s \gg u_A$ reduce to zero sound. Vortex motion also generates Alfvén and slow magnetosonic waves in the stellar crust. However, the intensity of radiation of those waves is small (in parameter u_A^3/u_s^3) as compared to the intensity of fast magnetosonic wave. Also Alfvén and slow magnetosonic waves are highly damped and can not reach the stellar surface. Due to these reasons we will not discuss radiation of Alfvén and slow magnetosonic waves.

Let us now consider excitation of electron zero sound by vortices in detail (see Fig. 2). Helical waves produce oscillation of the neutron vortex and, therefore, oscillation of protons in the *npe* phase. In *Aen* phase there is no drag effect and no electric current is produced by neutron vortices. For helical vortex motion the superfluid velocity of neutrons is

$$\mathbf{V}_n = \nabla\chi = \frac{\hbar}{2m_n r} \hat{\phi} + \mathbf{V}'_n$$

where $\mathbf{V}'_n = \nabla\chi'$ is the correction to the velocity due to the helical vortex motion,

$$\chi' = iA \frac{\hbar}{2m_n r} \exp [i(\omega t + k_{\parallel} z - \phi)]. \quad (17)$$

In the *npe* phase at $r < \Lambda$, where Λ is the screening length, the induced proton velocity around the neutron vortex is given by (Alpar et al. 1984):

$$\mathbf{V}_p \approx \frac{\delta m_p^*}{m_p^*} \mathbf{V}_n = \frac{\delta m_p^*}{m_p^*} \frac{\hbar}{2m_n r} \hat{\phi} + \mathbf{V}'_p(t), \quad (18)$$

where $\mathbf{V}'_p = \delta m_p^* \mathbf{V}'_n / m_p^*$. The last term in (18) is time dependent and produces density oscillation of protons according to the continuity equation

$$\frac{\partial \rho_p}{\partial t} = -\rho_p \text{div} \mathbf{V}'_p. \quad (19)$$

One should note that only z component of \mathbf{V}'_p contributes to the density oscillation since $\text{div} \mathbf{V}'_{p\perp} = 0$. The Debye length for electrons, $\Lambda_e = \sqrt{m_e c^2 / 4\pi e^2 n_e}$, is much less than characteristic scales of the proton density variation. As a result, free electrons screen the electric field produced by the moving protons, that is average electron velocity is approximately equal to the oscillating part of the proton velocity. In *Aen* phase there is no drag effect and electron motion is not coupled with neutron vortices.

We will assume that the core-crust interface is transparent for electrons and they can freely move from one phase into another. The assumption is reasonable since the electron Fermi energy is much larger than any Coulomb barrier that might exist at the interface over the interparticle scale. At the interface the oscillating electron motion generates zero sound waves which propagate across the stellar crust. To estimate the power of the radiated sound one can use the following simple analysis. We note that kinetic energy of ultrarelativistic electrons at the crust bottom is much larger than their interaction energy (Fermi gas

becomes more ideal with increasing its density). Therefore, the radiated power of zero sound should be approximately the same as in the limiting case of non interacting electrons. In this limit, the electrons move in a ballistic regime and the energy flux across the crust-core interface is given by

$$Q = \int E_e v_F dS, \quad (20)$$

where $v_F \approx c$ is the electron Fermi velocity and E_e is the contribution to the electron energy density due to the helical vortex motion. The integral in Eq. (20) is the surface integral over the interface. Eq. (20) takes into account that only electrons that move along the vortex line are coupled with the helical vortex motion and carry its energy. The rest electrons can not be excited by the helical wave because it would mean energy radiation by the helix in a perpendicular plane which is not possible (see Sec. 2.1).

As we have shown above, see Eq. (10), for a vortex in a single component superfluid the change in kinetic energy of neutrons determines the energy of the helical wave. However, this is not the case for a neutron vortex in the stellar core. Due to the drag effect the helical vortex motion inevitably produces density oscillation of superconducting protons and normal electrons (as we have mentioned in Sec. 2.2 the drag is very strong). As a result, the density oscillation of electrons (which is accompanied by large change in their Fermi energy) gives the main contribution to the helix energy in the stellar core and, hence, the energy of the helical wave is equal to $\int E_e L dS$, where L is the vortex length.

Taking into account Eq. (20), we obtain the following average energy flux of zero sound waves produced by a helical wave of a single vortex:

$$Q_1 = \frac{c}{L} \int E_e L dS = \frac{c}{L} \frac{\hbar\omega}{[\exp(\hbar\omega/k_B T) - 1]}. \quad (21)$$

One should note that the wave length of a sound is much larger than the size Λ of the area from which it is generated. Therefore, the sound wave has approximately a spherical front (which is similar to diffraction of light on a small orifice).

The number of vortex modes within the interval dk_{\parallel} is equal to $Ldk_{\parallel}/2\pi = L\sqrt{2m_n}d\omega/2\pi\sqrt{\hbar\omega \ln(\omega_c/\omega)}$ and, therefore, the spectral power density of sound waves produced by a single vortex line is

$$P_1(\omega) = \frac{c\sqrt{\hbar m_n \omega}}{\sqrt{2\pi}\sqrt{\ln(\omega_c/\omega)} [\exp(\hbar\omega/k_B T) - 1]}. \quad (22)$$

Eq. (22) is a universal expression that actually depends only on the core temperature T and the neutron mass m_n . Multiplying Eq. (22) by the number of neutron vortices in the superfluid $N = 2m_n R^2 \Omega / \hbar$ and dividing by 2π , we obtain the spectral density of sound waves power radiated from the oscillating vortex lattice in unit solid angle

$$P_v(\omega) = \frac{cm_n^{3/2} R^2 \Omega \sqrt{\omega}}{\sqrt{2\pi^2} \sqrt{\hbar \ln(\omega_c/\omega)} [\exp(\hbar\omega/k_B T) - 1]}, \quad (23)$$

where T is the temperature of the NS core.

Fast magnetosonic waves generated by vortices at the core-crust interface propagate across the stellar crust toward the surface. Along the wave propagation the properties of medium do not change very much over the length of the wave and the approximation of geometric acoustics is valid. The energy propagates along the rays and in the absence of absorption the energy flux remains constant along the direction of the ray, while properties of the medium slowly vary in space.

3. Attenuation of fast magnetosonic waves in the stellar crust

In this section we estimate attenuation of fast magnetosonic waves propagating across the stellar crust. We assume that crust matter is everywhere in a crystal phase: $T < T_m$, where T_m is the melting temperature. For iron crust $T_m = 2.5 \times 10^7 \rho_6^{1/3} \text{K}$, where ρ_6 is the matter density in units 10^6g/cm^3 (Hernquist 1984). Near the stellar surface there is a phase transition between a gaseous atmosphere and a condensed metallic phase. For iron the critical temperature of the phase transition can be estimated as $T_{\text{crit}} \sim 10^{5.5} H_{12}^{2/5} \text{K}$, where $H_{12} = H/10^{12}$, which is larger than the surface temperature ($\sim 10^6 \text{K}$) for strong enough magnetic field. We also assume that the atmosphere above the condensed surface has negligible optical depth which is the case when $T \lesssim T_{\text{crit}}/3$ (Lai 2001). Under such conditions electromagnetic radiation propagates through the atmosphere without damping. In Appendix C we study in detail attenuation of electromagnetic waves in hydrogen atmosphere and show that atmosphere is transparent for electromagnetic radiation if the density at the atmosphere bottom $\rho \lesssim 4 \text{g/cm}^3$. The density of the metallic phase at the stellar surface depends on magnetic field. E.g., for iron crust and $H = 10^{12} \text{Gs}$ the matter density at the crust surface is $\rho \approx 10^3 \text{g/cm}^3$ (Thorolfsson et al. 1998).

In our problem the speed of fast magnetosonic wave u is larger than the electron Fermi velocity (see Appendix B) and the speed of usual sound in the crystal lattice (phonons). Under such conditions the simple absorption processes (Landau damping) of a fast magnetosonic wave by electrons and phonons are not allowed due to a requirement of energy and momentum conservation. In Appendix A we discuss attenuation of zero sound and demonstrate that it is exponentially small for a weakly interacting Fermi gas, such as a gas of electrons in the NS crust and core (see Eq. (A9)). This contribution into attenuation comes from the collision integral in the kinetic equation. In the presence of magnetic field the electron sound is coupled with electromagnetic waves which results in another mechanism of damping. The point is that the fast magnetosonic waves are accompanied by oscillation of the electric field and in the presence of finite electrical conductivity σ the magnetosonic waves slightly dissipate energy. This contribution dominates and we discuss it in this section. To find the wave attenuation one should solve equations of magnetic hydrodynamics for electron motion with the resistive term (see Eq. (B12)), they are derived in Appendix B. As a result we obtain the following dispersion equation for the magnetosonic branch

$$\omega^2(\omega^2 - k^2 u_s^2) \left(1 - \frac{ic^2}{4\pi\sigma\omega} \left(k^2 - \frac{\omega^2}{c^2} \right) \right) - (\omega^2 - k_{\parallel}^2 u_s^2) \left(k^2 - \frac{\omega^2}{c^2} \right) u_A^2 = 0, \quad (24)$$

where $u_s \approx v_F$ is the speed of zero sound, $u_A = H/\sqrt{4\pi\rho_e}$ is the Alfvén velocity, ρ_e is the electron density and k_{\parallel} is the component of the wavevector along the magnetic field \mathbf{H} .

In the metallic crust the scattering of electrons on phonons is the dominant electron scattering mechanism. We will not discuss scattering on impurities since strong gravitational field produces space separation of nuclei with different masses during the “hot” stage of crust evolution. As a result, concentration of nuclei with different charges immersed in lattice sites is expected to be negligible. Effect of magnetic field on electron scattering is negligible unless the system as a whole occupies only a small number of Landau levels. Quantitatively this condition means that the number of levels populated is less than about 10 (Hernquist 1984). For iron lattice, the condition is equivalent to

$$\rho_6 < 0.6 H_{12}^{3/2}. \quad (25)$$

When condition (25) is satisfied the electron motion becomes effectively one dimensional. However, in 1D the simple electron-phonon scattering is not allowed because it is impossible to satisfy equations of energy and momentum conservation. Therefore, at densities given by Eq. (25) the electron scattering and magnetosonic

attenuation is suppressed by magnetic field. The wave attenuation can be substantial at larger densities where many Landau levels are populated and the magnetic field does not suppress the electron scattering. Let us now focus on this region. In this region the electron Fermi momentum is given by $p_F \approx \hbar(3\pi^2 n_e)^{1/3}$ and the Alfvén velocity u_A is smaller than $u_s \approx v_F$ (which is the case when $\rho_6 > 0.16 H_{12}^2 A/Z$, where Z is the nuclear charge, A is the atomic mass number).

At $u_A \ll u_s$ we obtain from Eq. (24) the following correction to the frequency of fast magnetosonic wave

$$\omega = ku_s + \frac{i(c^2 - u_s^2)^2 \omega^2 u_A^2 \sin^2 \theta}{8\pi\sigma u_s^4 c^2}, \quad (26)$$

where θ is the angle between the wavevector \mathbf{k} and the magnetic field \mathbf{H} , $u_s \approx v_F$ is the speed of the wave. The wave propagates without damping a distance l which depends on electron conductivity:

$$l \approx \frac{u_s}{\text{Im}\omega} = \frac{8\pi\sigma u_s^5 c^2}{\omega^2 (c^2 - u_s^2)^2 u_A^2 \sin^2 \theta}. \quad (27)$$

In the presence of magnetic field the electron conductivity can be estimated as (Kittel 1968)

$$\text{Re} \frac{1}{\sigma_{\perp}} = \text{Re} \frac{1}{\sigma_0} \left(1 + \frac{\omega_{He}^2}{\omega^2 + \nu_{\text{eff}}^2} \right), \quad \text{Re} \frac{1}{\sigma_{\parallel}} = \text{Re} \frac{1}{\sigma_0}, \quad (28)$$

where $\sigma_0 \approx e^2 c^2 n_e / E_F \nu_{\text{eff}}$ is the static conductivity without magnetic field, $\omega_{He} = eHc/E_F$ is the electron cyclotron frequency, $E_F = \sqrt{m_e^2 c^4 + c^2 p_F^2}$ is the electron Fermi energy, ν_{eff} is the effective frequency of electron collisions, σ_{\perp} , σ_{\parallel} are conductivities across and along the field \mathbf{H} . In magnetosonic waves the oscillating electric field is perpendicular to the magnetic field \mathbf{H} . Therefore, σ_{\perp} should be used to estimate the attenuation.

Also in the considering density region the crust temperature is much less than the Debye temperature (Kittel 1968)

$$T_D = \frac{(6\pi^2 n_i)^{1/3} \hbar c_s}{k_B} = 9.7 \times 10^7 \rho_6^{1/2} \frac{Z^{2/3}}{A} \text{K}, \quad (29)$$

where c_s is the speed of usual sound, n_i is the ion concentration. In the limit $T \ll T_D$ there are two effective frequencies of electron-phonon collisions (Lifshitz & Pitaevskii 1979). One of them $\nu_{1e,\text{ph}}$ describes energy relaxation (fast relaxation) and responsible for thermal conductivity in the absence of magnetic field

$$\nu_{1e,\text{ph}} \sim \frac{k_B T}{2\pi\hbar} \left(\frac{T}{T_D} \right)^2 = \frac{2 \times 10^{12} T_6^3 A^2}{\rho_6 Z^{4/3}} \text{s}^{-1}. \quad (30)$$

The other one $\nu_{2e,\text{ph}}$ describes slow relaxation of electrons in momentum directions and determines electrical conductivity

$$\nu_{2e,\text{ph}} \sim \frac{k_B T}{2\pi\hbar} \left(\frac{T}{T_D} \right)^4 = \frac{2 \times 10^9 T_6^5 A^4}{\rho_6^2 Z^{8/3}} \text{s}^{-1}. \quad (31)$$

Using Eqs. (27), (28), (31) in the limit $\nu_{\text{eff}} \ll \omega \ll \omega_{He}$ we obtain for ultrarelativistic electrons (that is when $\rho_6 > A/1.03Z$) the following expression for the free path of fast magnetosonic waves

$$l \approx \frac{8\pi c^9 n_e e^2}{(c^2 - v_F^2)^2 u_A^2 \omega_{He}^2 E_F \nu_{2e,\text{ph}} \sin^2 \theta} \approx \frac{1.14 \times 10^3 \rho_6^{17/3} Z^{19/3}}{H_{12}^4 T_6^5 A^{23/3} \sin^2 \theta} \text{cm}. \quad (32)$$

The matter density at the stellar crust ρ as a function of the distance to the surface h can be obtained from the condition that hydrostatic pressure $\int \rho g dh$ is equal to the pressure of electrons (here g is the acceleration of gravity). The pressure of ultrarelativistic electron gas is given by

$$P = \frac{(3\pi^2)^{1/3}}{4} \hbar c n_e^{4/3} = \frac{(3\pi^2)^{1/3} \hbar c}{4m_p^{4/3}} \rho^{4/3} (Z/A)^{4/3} \quad (33)$$

and we estimate

$$h = \frac{(3\pi^2)^{1/3} \hbar c \rho^{1/3}}{g m_p^{4/3}} \left(\frac{Z}{A}\right)^{4/3} = \frac{492 \rho_6^{1/3}}{g_{15}} \left(\frac{Z}{A}\right)^{4/3} \text{ cm}. \quad (34)$$

Fast magnetosonic waves propagate across the stellar crust without attenuation if at any density $l > h$. The attenuation increases with decreasing the matter density. Therefore, the maximum damping occurs in the boundary region where magnetic field still does not suppress the electron scattering. According to Eq. (25), in the region of maximum damping $\rho_6 \approx 0.6 H_{12}^{3/2}$ (the region is located several meters below the surface). Then using Eqs. (32), (34) we obtain the following condition at which waves pass the critical region and reach the stellar surface without attenuation (for ^{56}Fe lattice):

$$|\sin \theta| < \frac{0.004 H_{12}^2 g_{15}^{1/2}}{T_6^{5/2}}. \quad (35)$$

For $T = 10^6 \text{K}$, $H = 4 \times 10^{12} \text{Gs}$ and $g = 10^{15} \text{cm/s}^2$ only waves that in the critical region propagate along magnetic lines within the angle $|\theta| < 0.064 \text{rad} = 3.7^\circ$ (that is only about 0.2% of the total vortex radiation) reach the stellar surface without attenuation. However, with decrease of the surface temperature the angle θ becomes larger, e.g., if $T = 5 \times 10^5 \text{K}$, we obtain $|\theta| < 21^\circ$. Due to anisotropic attenuation the observed vortex radiation should be pulsed if magnetic poles are displaced from the axis of star rotation (like in pulsars). The radiation is maximum when the line of sight is close to the magnetic axis. According to Eq. (35), for colder NSs the shape of vortex pulse becomes broader.

4. Transformation of fast magnetosonic waves into electromagnetic radiation at the stellar surface

Let us consider the boundary between the stellar crust and atmosphere. One can approximately treat the atmosphere as a vacuum because its density is much less than density of the crust. When a magnetosonic wave incidents on the boundary, it undergoes partial reflection and partially transforms into electromagnetic wave which propagates into the vacuum. The relation between the waves is determined by the boundary conditions at the surface of separation, which require the tangential component of the electric field and the normal component of the magnetic field to be equal. Conservation of the energy flux imposes another boundary condition (Landau & Lifshits 1960):

$$\left[P + \frac{(H_t^2 - H_n^2)}{8\pi} \right] = 0, \quad (36)$$

where $P = P_0 + u_s^2 \rho'$ is the pressure, ρ' is the density oscillation of electron quasiparticles, H_t and H_n are tangential and normal components of the magnetic field. The square brackets denote the difference between the values on the two sides of the surface. From Eq. (36) we obtain the following condition for the oscillating part of the magnetic field \mathbf{h} and the density ρ' :

$$\left[u_s^2 \rho' + \frac{H_t h_t}{4\pi} \right] = 0, \quad [h_n] = 0. \quad (37)$$

The problem can be substantially simplified because near the stellar surface the Alfvén velocity is much larger than the speed of sound $u_A \gg u_s$. For $H = 10^{12}$ Gs, $\rho_e = 10^3(m_e/m_p)\text{g/cm}^3$ we obtain $u_A = 4 \times 10^{11}\text{cm/s} \gg c$. In this case the second term in Eq. (37) is in the factor $u_A^2/u_s^2 \gg 1$ greater than the pressure oscillation $u_s^2\rho'$ and the boundary condition reduces to $[h_t] = 0$. Also, under the condition $u_A \gg u_s$ the fast magnetosonic wave propagates with the velocity $u = u_A/\sqrt{1 + u_A^2/c^2}$ which is independent of the wavevector \mathbf{k} (see Eq. (B23)). The particle velocity \mathbf{V} in the wave lies in the kH plane and perpendicular to \mathbf{H} , while oscillating magnetic \mathbf{h} and electric fields \mathbf{E} are perpendicular to each other and \mathbf{k} :

$$\mathbf{E} = \frac{u_A}{\sqrt{c^2 + u_A^2}}(\mathbf{h} \times \hat{k}), \quad (38)$$

where \hat{k} is a unit vector in the direction of \mathbf{k} (see Fig. 3). We obtain that the fast magnetosonic wave near the stellar surface is similar to an electromagnetic wave in a medium with the dielectric constant $\varepsilon = 1 + c^2/u_A^2$ and the boundary conditions at the interface coincide with those for electric and magnetic field at the boundary of the dielectric medium. Therefore, transformation of the fast magnetosonic wave into electromagnetic one is described by the same formulas as refraction of electromagnetic waves at the interface between the dielectric and vacuum.

For example, let us consider the case when the magnetic field \mathbf{H} lies in the plane of incident wave. Then, the oscillating electric field \mathbf{E} is perpendicular to the plane of incidence. The transmission coefficient is given by

$$\tau = \frac{\sin(2\theta_1) \sin(2\theta_2)}{\sin^2(\theta_1 + \theta_2)}, \quad (39)$$

where θ_1 is the angle of incidence and θ_2 is the angle of refraction ($\sin \theta_2 = \sqrt{\varepsilon} \sin \theta_1$). For normal incidence ($\theta_1 = 0$) the transmission coefficient is

$$\tau = \frac{4\sqrt{\varepsilon}}{(\sqrt{\varepsilon} + 1)^2} = \frac{4\sqrt{1 + c^2/u_A^2}}{(\sqrt{1 + c^2/u_A^2} + 1)^2}. \quad (40)$$

If $u_A \gg c$ (which is the case when $H > 10^{11}$ Gs) the magnetosonic wave is completely transformed into electromagnetic wave ($\tau \approx 1$). In the opposite limit $u_A \ll c$ the transmission coefficient is small and $\tau \approx 4u_A/c$. Fig. 4 shows the general scheme of the vortex mechanism of NS radiation.

5. Spectrum of neutron star radiation

The spectral density of sound waves power radiated from the stellar core in unit solid angle is given by Eq. (23). However, as we have shown, only a fraction of magnetosonic waves that in the critical region propagate in the direction close to the magnetic lines reaches the stellar surface and only a fraction is transformed into electromagnetic waves which propagate into surrounding space. The fraction depends, in particular, on magnetic field strength and its distribution over the stellar surface.

Now let us discuss the region of applicability of Eq. (23). There is a fundamental limitation that affects the spectrum of vortex radiation in the infrared band. The limitation is that at any frequency the electromagnetic radiation produced by vortices should not exceed black body radiation produced by the surface $4\pi R^2$ with the same temperature T . This statement is one of the formulations of Kirchhoff's law which is a consequence of general thermodynamic principles. We assume that vortices are excited thermally and if at some frequency the vortex radiation becomes comparable with radiation of a black body this means

that at such frequency the rate of thermal excitation imposes the main restriction on the radiated power: vortices radiate maximum power which can be pumped from the thermal reservoir. Kirchhoff's law results in the following limitation on the frequency at which Eq. (23) describes the spectrum of electromagnetic radiation produced by vortices:

$$\frac{\omega}{2\pi} > \frac{0.24c^{6/5}m_n^{3/5}\Omega^{2/5}}{\hbar^{3/5}\ln^{1/5}(\omega_c/\omega)}, \quad (41)$$

where $\omega_c = \hbar/4m_n\xi^2 \approx 10^{20}\text{Hz}$. For $\Omega/2\pi = 4\text{s}^{-1}$ we obtain $\omega/2\pi > 1.5 \times 10^{14}\text{Hz}$. At lower frequencies the spectrum of vortex radiation (in unit solid angle) follows Planck's formula

$$P_v(\omega) = \frac{\hbar\omega^3 R^2}{4\pi^2 c^2 [\exp(\hbar\omega/k_B T) - 1]} \approx \frac{\omega^2 R^2 k_B T}{4\pi^2 c^2}, \quad (42)$$

where T is the temperature of the NS core.

One should mention that Eq. (41) for the kink frequency contains no free parameters. To take into account the gravitation redshift z one should divide Eq. (41) by $1+z$. Consequently, the observation of the kink in the infrared band allows measurement of the gravitation redshift at the core surface.

To compare our theory with available spectrum observations in different frequency bands it is convenient to represent the spectral density of vortex radiation $P_v(\omega)$ as a power law $P_v(\omega) \propto \omega^\alpha$, where α is the spectral index. The $\sqrt{\ln(\omega_c/\omega)}$ function in the denominator of Eq. (23) shifts the spectral index by a small value $1/2 \ln(\omega_c/\omega)$. The shift depends weakly on ω and changes the spectral index of vortex radiation from $\alpha \approx -0.46$ in the optical band to $\alpha \approx -0.43$ in the X -ray band.

Apart from vortex contribution there is thermal radiation from the NS surface, which for middle-aged pulsars dominates in the ultraviolet and soft X -ray bands. One should note that spectrum of thermal radiation may substantially differ from a black body. E. g., this is the case for NS atmospheres composed from light elements (hydrogen, helium) (Romani 1987). However, despite of the big difference, the observed thermal spectrum can be well fitted with a hydrogen (helium) atmosphere model as well as with a black body spectrum (Yakovlev et al. 1999a). The point is that spectrum of thermal radiation is usually detected only in the soft X -ray band. No data are available in the ultraviolet band due to strong interstellar absorption. In the soft X -ray band one can successfully fit the data assuming two black body components: hot polar caps and contribution from the rest (colder) NS surface. In the case of hydrogen (helium) atmosphere the data are well fitted with only one component contribution. In the optical-ultraviolet band the two models predict substantially different spectra and the hydrogen (helium) atmosphere curve lies above the black body giving the intensity several times greater. However due to the lack of data in this spectral region it is difficult to choose the adequate atmosphere model.

In this paper we estimate thermal radiation assuming helium atmosphere and use the numerical results obtained by Romani (Romani 1987). The model fits well the thermal spectrum with only one free parameter (the effective surface temperature T_{eff}). However, the main reason for choice of helium atmosphere is that if there is vortex radiation from the stellar surface then the atmosphere, in principle, can not be a black body because black body surface layer would absorb all passing radiation. From this point of view the detection of vortex radiation is a strong argument against black body atmosphere models.

The total radiation from a NS is given by the sum of vortex (Eqs. (23), (42)) and thermal components:

$$P(\omega) = aP_v(\omega) + P_{\text{th}}(\omega), \quad (43)$$

where $P_{\text{th}}(\omega)$ is the spectrum of surface thermal radiation. In Eq. (43) we introduced a dimensionless parameter a . The parameter is useful when we compare theoretical predictions with radiation observed from

pulsars. The free parameter a takes into account partial absorption of the vortex radiation near the stellar surface, geometrical effects related to unknown magnetic field distribution and position of the line of sight with respect to the cone swept by star’s magnetic axis. According to Eq. (35), for typical parameters of NSs and the surface temperature $T_s \approx 10^6\text{K}$ only about 0.2% of vortex radiation reaches the stellar surface and transforms into electromagnetic waves. However, the outgoing radiation is concentrated in a small solid angle near the magnetic axis which is determined by distribution of magnetic field. For typical pulse shapes this angle is of the order of 0.1rad. That is parameter a should be of the order of $0.002 \cdot 2\pi/0.1 \approx 0.1$. However, according to Eq. (35), with decreasing the surface temperature the parameter a increases as $a \propto 1/T_s^5$ and for colder NSs becomes of the order of 1.

In next section we compare the vortex radiation for different NSs with the thermal surface contribution. In such relative comparison the neutron star radius R_s (which is approximately equal to the core radius R) cancels in equations. As a result, in estimates there are only two free parameters: the core temperature T and the geometrical factor a . The effective surface temperature T_{eff} is directly determined from the thermal spectrum.

6. Discussion

Since the discovery of pulsars in 1967 numerous attempts were made to detect radiation from a NS surface. Observations were mainly successful in soft X –ray band because of high thermal luminosity in this region. Recent observations with ROSAT ($0.24 - 5.8 \times 10^{17}\text{Hz}$), ASCA ($0.17 - 2.4 \times 10^{18}\text{Hz}$) and Chandra obtained a detailed spectral information of a number of pulsars at X –ray energies. Only a few pulsars were observed in optical and ultraviolet bands and only some of them have detectable emission in these bands. In Fig. 5 we compare the observed radiation spectrum of middle-aged pulsars PSR B0656+14 ($\Omega/2\pi = 2.6\text{s}^{-1}$) and Vela ($\Omega/2\pi = 11.2\text{s}^{-1}$) with the radiation spectrum predicted by our theory. Thermal radiation of the stellar surface dominates in the ultraviolet and soft X –ray bands. We assume helium atmosphere with the effective surface temperature $T_{\text{eff}} = 4.9 \times 10^5\text{K}$ for PSR B0656+14 and $T_{\text{eff}} = 7.8 \times 10^5\text{K}$ for Vela. The NS radius R_s is related to the pulsar distance D : $R_s/10\text{km} = 5.28\sqrt{1+z}(D/1\text{kpc})$ for PSR B0656+14 and $R_s/10\text{km} = 4.1\sqrt{1+z}(D/1\text{kpc})$ for Vela (z is the NS redshift). For PSR B0656+14 and $D = 0.25\text{kpc}$ we obtain $R_s \approx 13\sqrt{1+z}\text{km}$, while for Vela and $D = 0.35\text{kpc}$ the surface radius is $R_s \approx 14\sqrt{1+z}\text{km}$. The vortex contribution (dash line) dominates in the infrared, optical and hard X –ray bands, where its spectrum has a slope $\alpha \approx -0.45$. In the far infrared band vortices radiate the maximum power which can be pumped by thermal excitation. In this band the radiation spectrum changes its behavior and follows Planck’s formula with $P(\omega) \propto \omega^2$. The sum of the vortex and thermal components is displayed with the solid line in Fig. 5. For PSR B0656+14 we take the core temperature $T = 6.4 \times 10^8\text{K}$ and the geometrical factor $a = 0.18$, while for Vela $T = 8 \times 10^8\text{K}$ and $a = 0.33$. The observed broad-band spectrum is consistent with our model for typical NS parameters. This suggests that the vortex mechanism of radiation operates in a broad frequency range from IR to hard X –rays. One should mention that the measured IR–optical spectrum has nonmonotonic behavior, which probably indicates the presence of unresolved spectral features or could be partially due to contamination of the pulsar flux by the nearby extended objects (Koptsevich et al. 2001). The slope of the non-thermal component is less steep than it was deduced by Pavlov et al. 1997 and Kurt et al. 1998 based on the optical–UV data only. Also, in the optical band the radiation of middle-aged pulsars was found to be highly pulsed with pulses similar to those in the hard X –ray band (Shearer et al. 1998; Shearer et al. 1997). This agrees with the vortex mechanism which predicts pulsed radiation.

In Fig. 6 we plot the broadband spectrum of the Geminga pulsar ($\Omega/2\pi = 4.2\text{s}^{-1}$) in optical– X –

ray bands. Solid line is the fit by the sum of the vortex and thermal contributions. In calculations we take $T_{\text{eff}} = 2 \times 10^5 \text{K}$, $T = 3 \times 10^8 \text{K}$ and $a = 0.22$. The radius of the Geminga pulsar is: $R_s/10\text{km} = 5.21\sqrt{1+z}(D/1\text{kpc})$, which for $D = 0.16\text{kpc}$ gives $R_s \approx 8.3\sqrt{1+z}\text{km}$. Our fit reasonably agrees with the observed spectrum apart from the dips in the IR-optical bands which probably appear due to ion cyclotron absorption (Martin et al. 1998). Also there is strong scattering of the data in the hard X -ray band which makes difficult comparison with the theory and, hence, estimates are less reliable. The data scattering might indicate on unresolved emission and absorption lines in this spectral region.

It is worth to note that the formula for vortex radiation contains two free parameters (T and a). As a result we can not determine each of these parameters separately from the observed fluxes, only their combination. However, the spectral index of vortex radiation is a fixed parameter in our theory. If a single mechanism of nonthermal radiation operates in the broad range, then the continuation of the X -ray fit to the optical range determines the spectral index of the nonthermal component with a big accuracy. Good quantitative agreement of our theory with the observed spectral index serves as a strong evidence that the vortex mechanism is responsible for radiation of middle-aged NSs in the IR, optical and hard X -ray bands. Also, there is an evidence of vortex contribution in radiation of young Crab pulsar. In optical band an emission during the “bridge” phase interval has been detected from the Crab with the spectral index $\alpha_{\text{opt}} = -0.44 \pm 0.19$ (Golden et al. 2000). The index differs from the flat spectrum of the peaks and can indicate on the vortex component.

Moreover, according to Eq. (23), the vortex contribution exponentially decreases at $\hbar\omega > k_B T$. Observation of such spectrum behavior allows us to determine directly the temperature of the stellar core T and can be a possible test of our mechanism. For PSR B0656+14 and the Vela pulsars the power law spectrum in the hard X -ray band shows no changes up to the highest frequency $2 \times 10^{18}\text{Hz}$ at which the data are available (see Fig. 5). According to our theory, this indicates that temperature of the NSs core is larger than $2 \times 10^8 \text{K}$. Measurements of spectra of middle-aged pulsars in the 10^{18} - 10^{19}Hz range are needed to search for possible manifestations of the core temperature.

One should note that recent observation of the Vela pulsar with the Rossi X -ray Timing Explorer has covered the energy band $2 - 30\text{keV}$ ($0.49 - 7.3 \times 10^{18}\text{Hz}$). These data in combination with OSSE observations ($70 - 570\text{keV}$) allows us to estimate the temperature of the Vela core. Light curves of the Vela pulsar have several peaks. We associate the vortex radiation with the second optical peak (see Fig. 1 in Harding et al. (1999) and Fig. 4 in Strickman et al. (1999)). In the ROSAT band ($0.06 - 2.4\text{keV}$) the vortex peak is weakly distinguishable on the background of strong thermal emission. However, the peak is clearly seen in the Rossi band in which thermal radiation is negligible. The peak becomes very small in the OSSE band and completely disappears at EGRET energies ($> 100\text{MeV}$). The vortex peak gives the main contribution to the average radiation intensity in the optical and hard X -ray bands and its spectral index agrees with our theory. One should note that in the Rossi band other peaks appear in the Vela light curves (Harding et al. 2002). Position of those peaks coincides with pulses at EGRET energies and, therefore, they have a different origin. The new peaks give the main contribution to the average radiation intensity at energy greater than 10keV . As a result, at such energies the average intensity carries no information about vortex radiation and a light curves study is necessary to separate the vortex contribution. To estimate the core temperature one should trace the evolution of the vortex peak in the energy interval $1\text{keV} - 1\text{MeV}$. According to Eq. (23), the frequency dependence of the peak amplitude depends only on the core temperature T . To our knowledge such analysis of the vortex peak amplitude has not been done yet. Nevertheless, it is possible to estimate the core temperature from available data. If we assume that the amplitude of the vortex peak follows Eq. (23), then we can find total (integrated over frequency) radiation intensities of vortices in different energy

bands. Then we compare the detected integrated intensities of the vortex peak in the Rossi and OSSE bands (Strickman et al. 1999) with those predicted by Eq. (23). We found that if there was no temperature decay of the vortex peak the total vortex intensity in the OSSE band should be three times larger than those actually observed. This indicates on the decay of the vortex spectrum and results in the following estimate of the core temperature of the Vela pulsar: $T \approx 8 \times 10^8 \text{K}$.

The temperature estimate ($T > 10^8 \text{K}$) allows us to make a conclusion about the interior constitution of the NSs. A hot NS cools mainly via neutrino emission from its core. Neutrino emission rates, and hence the temperature of the central part of a NS, depend on the properties of dense matter. If the direct Urca process for nucleons ($n \rightarrow p + e + \bar{\nu}_e$, $p + e \rightarrow n + \nu_e$) is allowed, the characteristic cooling time is $\tau_{Urca} \sim 1 \text{ min} / T_9^4$, where T_9 is the final temperature measured in units of 10^9K (Pethick 1992). Such neutron star cools to 10^8K in weeks. However, the characteristic age of PSR B0656+14 is about 10^5yrs , while the Vela pulsar is about 10^4 years old. So, the NS core cools down to 10^8K at least 10^6 times slower than the rate predicted by the direct Urca process. This estimate excludes equation of states incorporating Bose condensations of pions or kaons and quark matter. The point is that the neutrino emission processes for these states may be regarded as variants of the direct Urca process for nucleons (Pethick 1992). As a result, all these states give rise to neutrino emission, though generally smaller, comparable to that from the direct Urca process for nucleons which is inconsistent with the discrepancy of the cooling rate in the factor 10^6 . The conclusion about absence of exotic states of matter in the stellar core agrees with recent measurement of gravitational redshift from a NS (Cottam et al. 2002).

It is worth to mention here that dissipation of rotation kinetic energy in principle can produce heating of the stellar interior and supply energy for neutrino emission (Riper et al. 1995; Larson & Link 1999). Such possibility correlates with recent observation of emission properties of 27 pulsars by Becker and Trümper (1997) which suggests that pulsars radiation is emitted at the expense of their rotational energy (for $\Omega/2\pi = 10 \text{s}^{-1}$ the rotation energy $\sim M_\odot R_s^2 \Omega^2 \approx 10^{50} \text{erg}$). The superfluid core possesses the main part of the rotation kinetic energy, while radiation and dissipation of the angular momentum occurs from the stellar surface. As a result, the outer crust slows down faster than the superfluid core. The difference in the angular velocities between the superfluid and normal components causes friction which heats the core and transfers the angular momentum from the interior part to the outer crust. Superfluid vortices can play a crucial role in such process (Zhuravlev et al. 2001). One should note, however, that the neutrino emission rate comparable to that from the direct Urca process also contradicts to the rotation energy loss of NSs. Indeed, according to Lattimer et al. (1991), the neutrino emissivity in the direct Urca process is $Q_{Urca} \sim 10^{-27} T^6 \text{erg/s} \cdot \text{cm}^3$ and the total power radiated by neutrino at $T = 10^8 \text{K}$ is $P_{Urca} = \frac{4}{3} \pi R^3 Q_{Urca} \sim 4 \times 10^{39} \text{erg/s}$. This value is much larger than the rate of the kinetic energy loss of the middle-aged pulsars $10^{31} - 10^{36} \text{erg/s}$.

One should note that the characteristic time for cooling by the modified Urca process for normal nucleons is $\tau_{\text{modUrca}} \sim 1 \text{yr} / T_9^6$ (Pethick 1992). That is if the direct Urca process cannot occur, the core temperature will exceed $\sim 10^8 \text{K}$ for $\sim 10^6$ years. This result does not contradict the estimate $T > 10^8 \text{K}$ for middle-aged pulsars. However, more accurate determination of the core temperature of the Vela pulsar ($T \approx 8 \times 10^8 \text{K}$) demonstrates that NSs cool down much more slowly than could be explained by the modified Urca process for normal nucleons (such process would cool the core down to $8 \times 10^8 \text{K}$ during 4yrs, however the age of the Vela pulsar is about 10^4yrs). Possible explanation of this observation is that superfluidities of neutrons and protons in the stellar core are very strong so they substantially reduce all neutrino processes involving nucleons. If $k_B T \ll \Delta$, where Δ is the gap in the excitation spectrum of a superfluid, the modified Urca rates are reduced by a factor $\sim \exp(-2\Delta/k_B T)$. Using the measured value of the core temperature one can estimate the critical temperature of the superfluid transition. Theory predicts that in the stellar core the critical temperature of

the superconducting transition for protons T_{cp} is larger than the transition temperature of triplet neutron superfluidity T_{cn} (Hoffberg et al. 1970; Amundsen & Ostgaard 1985a; Amundsen & Ostgaard 1985b). As a result, the proton gap gives the main contribution to the suppression of neutrino emission by the modified Urca process. The corresponding reduction factors can be found in (Yakovlev et al. 2001). However, the appearance of neutron or proton superfluid initiates an additional specific neutrino production mechanism due to Cooper pair formation (Yakovlev et al. 1999b). Such mechanism of neutrino emission dominates until it dies out at $T < 0.1T_c$. The process involving superfluid neutrons $n \rightarrow n + \nu + \bar{\nu}$ is more important in the stellar core since their number greatly exceeds the number of protons. To find T_{cn} we assume 3P_2 triplet-state pairing of neutrons with the gap $\Delta = \Delta_0 \sqrt{1 + 3 \cos^2 \theta}$. The neutrino emissivity due to Cooper pairing of neutrons can be estimated using the result of Yakovlev et al. (1999b) $Q_{CP} = 2.2 \times 10^{-42} T^7 F(T/T_{cn}) \text{erg/s} \cdot \text{cm}^3$, where $F(x) \approx 1.27 \exp(-2.376/x)/x^6$ for $x \ll 1$. The stellar core cools down to the temperature T during the time $\tau = \int_T^\infty dTC(T)/Q_{CP}(T)$, where $C(T)$ is the specific heat. When $T \ll T_c$ the neutron (proton) contribution to the specific heat is exponentially small. Therefore, $C(T)$ is determined by the electron component $C(T) = (3\pi^2)^{2/3} n^{2/3} k_B^2 T / 3c\hbar$, where $n \approx 10^{38} \text{cm}^{-3}$ is the electron concentration in the stellar core. Using parameters of the Vela pulsar $T \approx 8 \times 10^8 \text{K}$, $\tau \approx 10^4 \text{yrs}$, we find the following critical temperature of triplet neutron superfluidity in the center part of the Vela core $T_{cn} \approx 9 \times 10^9 \text{K}$. Again one should mention the possibility of heating the stellar core by dissipation of the rotation energy. If such process is responsible for the Vela temperature than in equilibrium the heating rate is equal to the total power radiated by neutrino $(4/3)\pi R^3 Q_{CP}$. The kinetic energy loss of the Vela pulsar is $6.9 \times 10^{36} \text{erg/s}$ (Becker & Trümper 1997). If we assume that all kinetic energy loss goes in the neutrino emission than we obtain $T_{cn} \approx 6 \times 10^9 \text{K}$ ($R \approx 10 \text{km}$). The true value of T_{cn} lies between this estimate and the previous value $9 \times 10^9 \text{K}$ found under the assumption of no extra heating. More detailed analysis shows that the core temperature of middle-aged pulsars is probably maintained by the heating due to the dissipation of rotation energy. Our estimate of the critical temperature of neutron superfluidity agrees well with realistic nucleon-nucleon interaction potentials that fit recent world data for pp and np scattering up to 500MeV (Baldo et al. 1998). Such potentials give $T_{cn} \approx 7.5 \times 10^9 \text{K}$ at the density $2\psi_0$ that is expected at the center region of a canonical neutron star without exotic inner core, and predict $T_{cn} \approx 2 \times 10^9 \text{K}$ at the core-crust interface. One should mention that precise knowledge about nucleon-nucleon interaction at high energies (up to $\sim 2.5 \text{Gev}$) is a result of progress in accelerator physics during the last decade (Arndt et al. 1994; Arndt et al. 1997). Estimates of T_{cn} made in 1970's and 1980's usually substantially differ from the current value. E.g., Amundsen & Ostgaard (1985b) gave the maximum value of T_{cn} in the stellar core $T_{cn} = 9 \times 10^8 \text{K}$ which is almost one order of magnitude less than the current result. Recent experiments on nucleon-nucleon scattering favor in strong superfluidity and superconductivity in the stellar core, such observations are also supported by the theory (Elgaroy et al. 1996; Baldo & Grasso 2001).

It is worth to note that we may rule out the exotic states of matter only for NSs which display vortex radiation in the hard X -ray band. However it may not be the case for the whole NS population and a systematic study of pulsars radiation in the X -ray band is necessary. If exotic states do exist in some dense NSs the middle-aged pulsars with the core temperature $< 10^7 \text{K}$ could be candidates for stars with Bose condensates or quark matter.

7. Energy transport across the stellar crust

The theory of NS cooling has been developing over more than 30 years. First let us discuss the current understanding of temperature distribution in a crust of middle-aged NSs. The question is important because

NS cooling theory is used as a method to determine the core temperature from the surface temperature and, hence, to explore properties of superdense matter. In current theories it is assumed that high density of the stellar interior provides high thermal conductivity of internal layers. As a result, in about $10^2 - 10^3$ years after the star formation, a wide, almost isothermal region is formed within the entire core and the main fraction of the stellar crust (Yakovlev et al. 1999a). The isothermal stellar interior is surrounded by a very thin subphotospheric layer with thickness of the order of several meters. This low dense surface layer produces thermal isolation of the NS interior. The heat transport through the isolating layer determines the relation between the surface temperature T_s and the interior temperature T . In particular, T/T_s depends on the surface gravity and the chemical composition of the outer NS envelope. For $T_s = 5 \times 10^5 \text{K}$ and a nonmagnetized NS the ratio T/T_s typically lies in the interval $20 \div 100$ (Potekhin et al. 1997).

Possible presence of a strong magnetic field increases the uncertainty. The point is that magnetic field suppresses the electron thermal conductivity across the field lines and enhances along the lines. The effect of magnetic field on NS cooling has been studied by several authors. E.g., a relationship between the internal and surface temperatures in a NS with the magnetic field normal to the surface was investigated by Van Riper (1988). Page (1995) as well as Shibanov & Yakovlev (1996) considered the NS cooling with a dipole magnetic field.

As we have found based on spectra observations the effective surface temperature of the Vela Pulsar is $7.8 \times 10^5 \text{K}$, while the core temperature is about $8 \times 10^8 \text{K}$. This value of the core temperature is much larger than those predicted in heat transport models discussed in literature so far. The purpose of this section is to explain the big difference. Here we show that if near the core surface the magnetic field is parallel to the core it produces substantial heat isolation and can explain the big difference between the core and surface temperatures. Such assumption is simply a boundary condition for the magnetic field at the superconductor boundary. In this model the main temperature drop occurs in a thin layer near the crust bottom which differs from current cooling theories that predict isothermal inner crust.

Let us consider heat transport across the stellar crust in the presence of a strong magnetic field. We assume that free electrons give the main contribution to thermal conductivity. In the presence of a strong magnetic field ($E_F \gg \omega_{\text{He}} \gg \nu_e$) the electron thermal conductivity across the field can be estimated as

$$\kappa_{e\perp} \approx \frac{\pi^2 n_e c^2 k_B^2 T \nu_e}{3 E_F \omega_{\text{He}}^2}, \quad (44)$$

where ν_e is the frequency of electron relaxation in momentum directions which can be due to electron-phonon (Eq. (31)) or electron-electron collisions. At $T \ll T_F$, where T_F is the Fermi temperature, the frequency of electron-electron collisions for ultrarelativistic electrons is

$$\nu_{e,e} \sim \frac{e^4 n_e^{1/3}}{\hbar^2 c} \left(\frac{T}{T_F} \right)^2 = 3.2 \times 10^{18} \frac{T_6^2}{n_e^{1/3}} \text{s}^{-1}. \quad (45)$$

For $n_e = 10^{36} \text{cm}^{-3}$, $T = 10^8 \text{K}$ we obtain $\nu_{e,e} \approx 3.2 \times 10^{10} \text{s}^{-1}$. Near the crust-core interface $\nu_{e,e} > \nu_{2e,\text{ph}}$ and, therefore, $\nu_{e,e}$ should be substituted into Eq. (44). As a result, the electron thermal conductivity across the magnetic field is given by

$$\kappa_{e\perp} \approx 8.5 \times 10^{-29} \frac{n_e T_6^3}{H_{12}^2} \frac{\text{erg}}{\text{K} \cdot \text{cm} \cdot \text{s}}. \quad (46)$$

For $n_e = 10^{36} \text{cm}^{-3}$, $T = 10^8 \text{K}$, $H = 10^{12} \text{Gs}$ we obtain $\kappa_{e\perp} \approx 8.5 \times 10^{13} \text{erg/K} \cdot \text{cm} \cdot \text{s}$. Magnetic field suppresses $\kappa_{e\perp}$ in a factor $\nu_{e,e} \nu_{1e,\text{ph}} / \omega_{\text{He}}^2 \approx 10^{-11}$. One should mention that Eq. (46) is valid when $\omega_{\text{He}}^2 \gg \nu_{e,e} \nu_{1e,\text{ph}}$. In the opposite limit the magnetic field does not affect the thermal conduction.

Eq. (46) has to be compared with the phonon contribution to thermal conductivity which for $T \ll T_D$ can be estimated as (for phonon relaxation on electrons):

$$\kappa_{\text{ph}} \approx \frac{4\pi^3 k_B^3 T^2}{5\hbar^2 c} = 1.97 \times 10^9 T_6^2 \frac{\text{erg}}{\text{K} \cdot \text{cm} \cdot \text{s}}. \quad (47)$$

For $T = 10^8 \text{K}$ we obtain $\kappa_{\text{ph}} \approx 2 \times 10^{13} \text{erg/K} \cdot \text{cm} \cdot \text{s}$. At such temperatures, the electron thermoconductivity $\kappa_{e\perp}$ is still larger than κ_{ph} .

Now let us show that magnetic thermal isolation can substantially reduce the heat transport from the stellar core. Under such condition the magnetosonic waves produced by vortices can become the dominant mechanism of energy transfer to the stellar surface. The superconducting core expels magnetic field from its interior so that outside the core the magnetic lines are parallel to the superconductor boundary. As a result, near the crust bottom the magnetic field is tangential to the stellar core which produces substantial thermal isolation. To estimate the heat transfer across the magnetic layer we consider the following model. We assume that there is a strong magnetic field parallel to the core surface in a thin layer of width d . The width d is much less than the crust thickness ($d \ll 1\text{km}$). Outside the layer we assume the magnetic field to be weak or not tangential to the surface so that outside the layer the field does not suppress thermal conductivity across the crust.

One should also take into account that at high temperature the neutrino emission processes result in substantial energy loss and can affect the temperature profile in the inner crust. We assume that neutrino emission due to Cooper pairing of neutrons is the main mechanism of neutrino generation near the crust bottom. The process represents neutrino pair emission (of any flavor) by a neutron whose dispersion relation contains an energy gap: $n \rightarrow n + \nu + \bar{\nu}$ (Yakovlev et al. 1999b). In this process the main neutrino energy release takes place in the temperature range $0.2T_c \lesssim T \lesssim 0.96T_c$, where T_c is the critical temperature of neutron superfluidity. At densities near the crust bottom $T_c \approx 10^9 \text{K}$ and, therefore, the neutrino emission due to Cooper pairing of neutrons modifies the temperature distribution at $2 \times 10^8 \lesssim T \lesssim 10^9 \text{K}$. In this temperature range we assume the following neutrino emissivity $Q \approx 10^{22} T_9^8 \text{erg/s} \cdot \text{cm}^3$ (Yakovlev et al. 1999b).

Fig. 7 shows the temperature distribution in the NS crust as a function of the distance to the crust-core interface z . We take temperature at the crust-core interface $T = 8 \times 10^8 \text{K}$ (the Vela pulsar), the width of magnetic layer is $d = 50\text{m}$. Thermal conductivity across the layer is given by Eq. (46) with $n_e = 5 \times 10^{36} \text{cm}^{-3}$ and $H = 4 \times 10^{12} \text{Gs}$. Neutrino emission substantially modifies the temperature distribution and reduces the heat flux at $z < 40\text{m}$. At larger distances from the core the temperature becomes low enough so that neutrino emission is no longer important. In this region the heat flux is conserved. At $z > d$ the thermal conductivity is not suppressed by magnetic field and temperature remains approximately constant. Near the star surface (at distance less than 1m from the surface) there is another temperature drop due to substantial decrease of thermal conductivity at low densities. In estimates we take the crust width is equal to 1km. Practically all heat flux from the stellar core is lost by neutrino emission in a thin layer near the crust bottom. In our model the total energy losses of the stellar core due to thermoconductivity is $7 \times 10^{35} \text{erg/s}$ (for core radius $R = 10\text{km}$), while only $1.4 \times 10^{31} \text{erg/s}$ passes the magnetic layer and contribute to thermal radiation from the surface.

One should note that this value is about 20 times less than thermal energy actually radiated from the Vela surface: for $R_s = 10\text{km}$, $T_{\text{eff}} = 7.8 \times 10^5 \text{K}$ we obtain $4\pi R^2 \sigma T_{\text{eff}}^4 = 2.6 \times 10^{32} \text{erg/s}$. Such big discrepancy allows us to advance a hypothesis that vortex radiation, rather than thermoconductivity, is the main mechanism of heat transfer to the stellar surface. To check the hypothesis let us estimate the temperature of a black body that radiates the same total power as radiated by vortices from the superfluid

core. Using Eq. (23) we obtain

$$T_{\text{eff}} = \frac{\hbar^{1/4} c^{3/4} m_n^{3/8} \Omega^{1/4} T^{3/8}}{k_B^{5/8} \ln^{1/8} (\hbar \omega_c / k_B T)}. \quad (48)$$

In our model the fast magnetosonic waves generated by vortices propagate practically across the whole crust in a ballistic regime. For not too cold NSs a thin layer near the stellar surface absorbs practically all magnetosonic waves apart from a small fraction which reaches the surface. If thermoconductivity across the crust is suppressed by magnetic field, then vortex radiation can become the main mechanism of energy transfer from the core to the surface. Under such condition the energy radiated by vortices should be equal to the thermal energy radiated from the stellar surface and Eq. (48) determines the effective surface temperature which is directly measured from observations in the soft X -ray band. One should note that Eq. (48) contains no free parameters because T_{eff} and T can be measured independently and an uncertainty in $\omega_c = \hbar/4m_n\xi^2$ under the logarithm might change the answer only in a few percents.

From observation of the Vela pulsar in the hard X -ray and soft γ -ray bands we estimated the Vela core temperature $T \approx 8 \times 10^8 \text{K}$. For this value of the core temperature, $\Omega/2\pi = 11.2 \text{s}^{-1}$ and $\omega_c/2\pi = 10^{20} \text{Hz}$ Eq. (48) gives $T_{\text{eff}} = 7.6 \times 10^5 \text{K}$, which approximately coincides with the effective surface temperature of the Vela pulsar obtained from observations of thermal spectrum in the soft X -ray band $T_{\text{eff}} = 7.8 \times 10^5 \text{K}$. Such excellent agreement with observations is remarkable because the theory contains no free parameters! This confirms our hypothesis that vortex radiation, rather than thermoconductivity, is the main mechanism of heat transfer to the stellar surface in middle-aged NSs (at least in some of them). Also such agreement is a strong argument in favor of the theory of vortex radiation.

As a result, one can use Eq. (48) to estimate the core temperature T of middle-aged NSs from their surface temperature T_{eff} and obtain the following practical relation:

$$T_8 \ln^{1/3} (48/T_8) = \frac{0.22 T_{\text{eff}5}^{8/3}}{(\Omega/2\pi)^{2/3}}. \quad (49)$$

For PSR B0656+14 $T_{\text{eff}} = 4.9 \times 10^5 \text{K}$, $\Omega/2\pi = 2.6 \text{s}^{-1}$ and Eq. (49) gives the core temperature $T \approx 6.4 \times 10^8 \text{K}$. For Geminga $T_{\text{eff}} = 2 \times 10^5 \text{K}$, $\Omega/2\pi = 4.2 \text{s}^{-1}$ and we obtain $T \approx 0.3 \times 10^8 \text{K}$. One should mention that for colder NSs (such as Geminga) absorption of vortex radiation near the surface becomes small (see Eq. (35)). In this case Eq. (49) is less reliable and can substantially underestimate the core temperature. For colder NSs with still strong magnetic field the total power of vortex radiation becomes larger than thermal surface emission.

8. Conclusions and outlook

In this paper we discuss a new possible mechanism of NS radiation produced by vortices in the superfluid core. The key idea is that neutron star interior is transparent for electron zero sound, the same way as it is transparent for neutrinos. The waves of zero sound (in electron liquid) are generated at the core-crust interface by superfluid vortices which undergo thermal helical oscillations. Sound waves produced by vortices propagate across the stellar crust towards the surface. In the presence of magnetic field sound is coupled with electromagnetic waves. Virtually, they are limiting cases of the same essence - the fast magnetosonic wave which is known in magnetic hydrodynamics. Near the crust bottom, where the density is large, the fast magnetosonic waves reduce to zero sound (the effect of magnetic field is negligible). However, near the stellar surface the Alfvén velocity becomes larger than the speed of sound and the fast magnetosonic waves behave as

electromagnetic waves in a medium. As a result, at the stellar surface the fast magnetosonic waves transform into electromagnetic radiation in vacuum the same way as refraction of usual electromagnetic waves at the dielectric-vacuum interface. For typical magnetic fields of the middle-aged NSs the transformation coefficient is close to 1.

Finite conductivity of the crust results in partial absorption of magnetosonic waves in a thin layer near the stellar surface. As a result, only a fraction of waves which in the absorbing layer propagate in the direction close to magnetic lines reach the surface and transform into electromagnetic radiation. The fraction depends on the magnetic field strength and surface temperature. For typical parameters of middle aged NSs the fraction is less than 1%, however for colder stars, such as Geminga, it can be substantially larger (even of the order of 100%). As a consequence of anisotropic attenuation and star rotation the observed vortex radiation is pulsed, pulse shape is broader for colder stars. The part of vortex radiation absorbed near the surface contributes to the heat transfer from the core to the surface. Estimates show that at least for some NSs such mechanism, rather than thermoconductivity, is the main source of heating the stellar surface.

Stellar radiation produced by vortices has the spectral index $\alpha \approx -0.45$ and for middle-aged pulsars dominates in the IR, optical and hard X -ray bands. While the thermal surface radiation contributes mainly in the ultraviolet and soft X -ray bands. The observed spectra of PSR B0656+14, Vela and Geminga pulsars agree with our theory. In particular, there is an excellent agreement with observations in two predictions where the theory contains no free parameters: the spectral index of vortex radiation α and the relation between the core and surface temperatures (given by Eq. (48)). There are also several predictions which have to be confirmed by future observations. For example, the theory predicts a kink of the vortex radiation spectrum in the infrared band (see Eqs. (41), (42) and Figs. 5,6) and an exponential decay of the spectrum in the hard X -ray band at $\hbar\omega > k_B T$ (see Eq. (23)) which was not measured in details yet.

The vortex radiation is produced in the stellar interior and contains important information about properties of the NS core, in particular, it allows direct determination of the core temperature. Comparing theory with available spectra observations we found that the core temperature of the Vela pulsar is $T \approx 8 \times 10^8 \text{K}$, which is the first measurement of the temperature of a neutron star core. It is important to note that the temperature we found is much larger than those predicted in heat transport models discussed in literature so far. To understand the big difference we consider heat transport in a model with magnetic field parallel to the core surface (which is just a boundary condition at the superconductor boundary) and show that the effect of magnetic thermal isolation can explain so high value of the core temperature as compared with the stellar surface temperature.

A direct measurement of the core temperature by means of detection the vortex radiation opens a new perspective in study superdense matter. In particular, our estimate of the interior temperatures of PSR B0656+14, Vela and Geminga pulsars rules out possibility of exotic states, such as Bose condensation of pions or kaons and quark matter, in these objects. Also it allows us to extract the superfluid transition temperature for neutrons in the center region of the stellar core $T_c = (7.5 \pm 1.5) \times 10^9 \text{K}$ which is the first determination of such parameter from observations.

Detection of vortex radiation opens a possibility to study composition of NS crust (NS interior spectroscopy). Since magnetosonic waves generated by vortices propagate through the stellar interior the spectrum of vortex radiation should contain (redshifted) absorption lines which correspond to low energy excitations of nuclei that form NS crust. E. g., the $^{57}_{26}\text{Fe}$ nucleus has an excited state with the energy $14.4 \text{keV} = 3.5 \times 10^{18} \text{Hz}$, which would produce an absorption line in the hard X -ray band of vortex radiation spectrum if temperature of the stellar core is greater than $1.7 \times 10^8 \text{K}$. The other possible absorption lines

in the X ray band can be produced by nuclei $^{45}_{21}\text{Sc}$ (12.4keV), $^{56}_{25}\text{Mn}$ (26keV), $^{73}_{32}\text{Ge}$ (13.5keV) or by heavy nuclei $^{235}_{92}\text{U}$ (13keV), $^{249}_{97}\text{Bk}$ (8.8keV). One should mention that bottom layers of neutron star crust may contain exotic nuclei with mass number up to about 600 and vortex radiation can be a possible tool to study their properties. However, the absorption lines of nuclei are narrow and large spectral resolution is necessary for their detection. If temperature of the stellar crust $T_{crust} \sim 10^8\text{K}$ the relative thermal line width is $\sqrt{2k_B T_{crust}/Mc^2} \approx 2 \times 10^{-5}$. Under such condition the star rotation gives the main contribution to the line broadening and the corresponding Doppler line width for middle-aged pulsars can be estimated as $\Omega R_s/c = 0.001 - 0.01$.

Another challenging goal for future study is interaction of zero sound with exotic states of matter which might exist in more dense NSs. The point is that generation of zero sound by vortices is only one of the possible mechanisms. If an exotic state of matter absorbs zero sound at some frequency, then, according to Kirchhoff's law, it will radiate zero sound at this frequency. As a result, spectrum of stellar radiation must contain characteristic emission lines corresponding to such processes which allows a direct spectroscopic study of superdense matter. In the limiting case when the inner core matter absorbs all zero sound waves the stellar radiation spectrum should be close to radiation of a black body with the temperature of the core. One should look for such objects among bright galactic X -ray sources. Also zero sound can be emitted in reactions between elementary particles that constitute the stellar core. It is known that some pulsars are powerful sources of γ -rays and it would be interesting to study the connection between γ radiation and zero sound. It is also interesting to investigate a possible connection between electron sound and nonthermal radiation of young (Crab like) pulsars which reveals flat spectrum in the optical band.

I am very grateful to A. Fetter, G. Shlyapnikov, M. Binger, S. T. Chui, V. Ryzhov for valuable discussions and the Aspen Center for Physics where part of the results has been obtained. This work was supported by the National Science Foundation, Grant No. DMR 99-71518 and by NASA, Grant No. NAG8-1427.

A. Zero sound in electron liquid

In 1957 Landau predicted existence of collective sound excitations in Fermi systems which exist in collisionless regime and called them “zero sound” (Landau 1957). Zero sound waves propagate with the speed u_s greater than the Fermi velocity v_F which excludes possibility of collisionless Landau damping. Later, zero sound was observed in liquid ^3He (Keen et al. 1965; Abel et al. 1966) and in electron liquid in metals (Burma et al. 1989; Bezuglyi et al. 1991; Bezuglyi et al. 1995). The appearance of zero-sound oscillations in charged Fermi liquids was studied by Silin (1958) and Gor'kov & Dzyaloshinskii (1963). In particular, Gor'kov & Dzyaloshinskii (1963) have shown that for weakly interacting electrons ordinary zero sound can be propagated in the directions of the symmetry axes in metals while spin zero sound apparently exists in any type of metal. As a consequence of collective motion the attenuation of zero sound can be atypically small compared to single particle excitations in Fermi liquids. E.g., in normal ^3He liquid under the pressure 27atm the attenuation length of longitudinal zero sound 2500 times exceeds the free path of single quasiparticles and the ratio substantially increases with increasing the pressure (Corruccini et al. 1969). For huge pressures, such as in a neutron star crust, it is reasonably to expect very small attenuation of collective modes.

Due to the presence of long-range Coulomb interactions, the Landau theory of Fermi liquid is not directly applicable to electron gas in metals. However, in electron gases the Coulomb interaction between

quasiparticles is screened by the gas polarizability and effectively becomes a short-range. It is therefore conceivable that density waves of quasiparticles could arise having a typical sound spectrum. If we take into account screening the effective interaction potential between quasiparticles in momentum space is given by

$$V_{\text{eff}}(\omega, \mathbf{k}) = \frac{4\pi e^2}{k^2 \varepsilon_l(\omega, \mathbf{k})}, \quad (\text{A1})$$

where $\varepsilon_l(\omega, \mathbf{k})$ is the longitudinal dielectric function. In random phase approximation (RPA) (Pines & Nozieres 1989)

$$\varepsilon_l(\omega, \mathbf{k}) = 1 - V(k)\chi^0(\omega, \mathbf{k}), \quad (\text{A2})$$

where $V(k) = 4\pi e^2/k^2$ is the interaction potential between bare electrons and $\chi^0(\omega, \mathbf{k})$ is the density-density response function for noninteracting fermions which is in the limit $k \ll k_F$, $\hbar\omega \ll E_F$ given by

$$\chi^0(\omega, \mathbf{k}) = \frac{3n}{2E_F} \left(\frac{\omega}{2v_F k} \ln \left(\frac{\omega + v_F k}{\omega - v_F k} \right) - 1 \right), \quad (\text{A3})$$

n is the electron concentration, v_F is the Fermi velocity. In this section we assume absence of external magnetic field. Hence, in RPA

$$V_{\text{eff}}(\omega, \mathbf{k}) = \frac{4\pi e^2}{\left[k^2 + q_{TF}^2 \left(1 - \frac{s}{2} \ln \left(\frac{s+1}{s-1} \right) \right) \right]}, \quad (\text{A4})$$

where $s = \omega/v_F k$, $q_{TF}^2 = 6\pi n e^2/E_F$ is the Thomas-Fermi screening wavevector. Such form of the interaction potential suggests screening of the electric charge. E.g., if $V_{\text{eff}}(k) = 4\pi e^2/(k^2 + q_c^2)$ the interaction potential in coordinate space has the form $V_{\text{eff}}(r) = (e^2/r) \exp(-q_c r)$, that is the effective quasiparticle interaction is short-range.

The RPA takes into account electron interaction only to the extent required to produce the screening field. The effects arising from interaction between screened charges (such as zero sound), are, therefore, beyond the RPA. One should note, however, that screening depends substantially on ω and k . For $\omega \gg v_F k$ ($s \gg 1$) the screening is small $V_{\text{eff}}(\omega, \mathbf{k}) \approx 4\pi e^2/(k^2 - q_{TF}^2/3s^2) \approx V(k)$ and, hence, RPA is a valid theory. This is the reason why RPA is successful in describing plasmons in metals for which $\omega \gg v_F k$. Indeed, the dispersion equation $\varepsilon_l(\omega, \mathbf{k}) = 0$ with $\varepsilon_l(\omega, \mathbf{k})$ given by (A2) has a solution $\omega^2 = 4\pi e^2 n/m_e$ corresponding to oscillations with plasma frequency.

However, in the region where zero sound branch is expected (for weakly interacting fermions this region is $s - 1 \ll 1$) Eq. (A4) predicts large screening and RPA can not capture collective modes in this region. Instead, one can apply a phenomenological Landau theory based on the effective screened interactions between quasiparticles. The Landau theory describes interaction by means of dimensionless phenomenological parameters F_l, G_l which measure the interaction strength as compared to the kinetic energy. The parameters F_l, G_l describe respectively the spin symmetric and spin antisymmetric parts of the quasiparticle interaction. For weakly interacting Fermi gas only the first two parameters F_0 and G_0 are relevant, they are related to each other by $G_0 = -F_0$ which is the property of exchange interaction between electrons. Parameters F_0 and G_0 describe propagation of axisymmetric (longitudinal) zero sound. Propagation of zero sound is possible when $F_0 > 0$ or $G_0 > 0$. The former case corresponds to an ordinary zero sound, while the latter one is known as spin zero sound in which oscillation of the quasiparticle distribution function depends on the spin direction. Loosely speaking F_0 describes propagation through the medium of a particle-hole pair with the total spin 0, while in the spin zero sound the total spin of the propagating particle-hole pair is equal to 1

(Gottfried & Pičman 1960). The speed of ordinary zero sound $u_s = sv_F$ is determined from the equation (Landau 1957)

$$\frac{s}{2} \ln \left(\frac{s+1}{s-1} \right) - 1 = \frac{1}{F_0}, \quad (\text{A5})$$

which for weakly interacting fermions $F_0 \ll 1$ reduces to

$$s - 1 \approx 2 \exp \left(-2 - \frac{2}{F_0} \right). \quad (\text{A6})$$

That is the speed of zero sound is exponentially close to v_F . The speed of spin zero sound is described by the same Eqs. (A5), (A6) with G_0 instead of F_0 . The property $G_0 = -F_0$ suggests that one of these parameters is positive. This is a manifestation of a general statement that ordinary or spin longitudinal zero sound exist in any stable Fermi liquid (Mermin 1967).

For a short-range weak interaction between fermions the Landau parameters can be expressed in terms of the interaction potential as $F_0 = 3nV_{\text{eff}}(k=0)/2E_F$. Formal application of Eq. (A4) at $k \rightarrow 0$, $s \rightarrow 1$ yields $F_0 = 2/\ln[(s-1)/2] < 0$, $|F_0| \ll 1$. This gives us a hint that F_0 has a small negative value. The magnitude of F_0 can be approximately estimated as the ratio of the Coulomb energy to the kinetic (Fermi) energy. For relativistic electron gas in the stellar crust we obtain: $F_0 \approx -e^2k_F/E_F = -1/\alpha = -0.007$, where $\alpha = c\hbar/e^2$ is the fine structure constant. Negative value of F_0 suggests that G_0 is positive ($G_0 = -F_0 \approx 0.007$) and, hence, the spin zero sound can propagate through the stellar crust.

Such conclusion can be justified by consideration of the density-density response function, for weakly interacting Fermi gas it is given by (Gottfried & Pičman 1960)

$$\chi_\lambda(\omega, \mathbf{k}) = \frac{\chi^0(\omega, \mathbf{k})}{1 - (-1)^\lambda V_{\text{eff}}(\omega, \mathbf{k})\chi^0(\omega, \mathbf{k})}, \quad (\text{A7})$$

where $\lambda = 0, 1$ is the total spin of the particle-hole pair which can be excited in a singlet ($\lambda = 0$) or a triplet state ($\lambda = 1$). Collective modes of the system are determined by the poles of $\chi_\lambda(\omega, \mathbf{k})$. If we take $V_{\text{eff}}(\omega, \mathbf{k})$ from Eq. (A4) then $\chi_\lambda(\omega, \mathbf{k})$ has a pole at $\omega = v_F k$ for $\lambda = 1$. This pole describes spin zero sound, while the plasmon branch corresponds to a pole for $\lambda = 0$. In such approach we find that speed of zero sound is exactly equal to v_F which corresponds to the limiting case of noninteracting quasiparticles. The result formally appears because $V_{\text{eff}}(\omega, \mathbf{k})$ vanishes at $s = 1$ which means infinite screening of Coulomb interaction. However, in real systems there is no screening at distances less than the interparticle spacing $\approx 1/k_F$, that is instead of zero one should take $|V_{\text{eff}}| \approx e^2k_F/n$. As a result, the position of the pole is shifted from $s = 1$ and determined by the same Landau expression (A5) with $G_0 \approx e^2k_F/E_F$. In Appendix B we discuss zero sound from the viewpoint of two component (particle-hole) picture of excitations in electron liquid.

A remarkable feature of zero sound in a weakly interacting Fermi gas is that its attenuation is exponentially small. Attenuation of zero sound occurs by means of excitation of two electron-hole pairs, since single particle processes (Landau damping) are not allowed ($u_s > v_F$). Gottfried and Pičman (1960) have solved the problem about zero sound attenuation in a weakly interacting Fermi gas for $T = 0$ and obtained the following result for the imaginary part of the sound frequency

$$\text{Im}\omega = (s - 1) \frac{\pi^4 \hbar \omega^2}{2E_F}. \quad (\text{A8})$$

For weak interactions the multiple $s - 1$ is exponentially small which provides exponentially small sound attenuation. Formal reason for this is the logarithmic singularity in the density-density response function

for noninteracting fermions $\chi^0(\omega, \mathbf{k})$ at $\omega = v_F k$ (see Eq. (A3)). Finite temperature can be immediately included using the Landau formula (Landau 1957), finally we obtain the free path length for zero sound

$$l = \frac{u_s}{\text{Im}\omega} = \frac{\hbar v_F E_F \exp(2 + 2/G_0)}{\pi^4 [(\hbar\omega)^2 + (2\pi k_B T)^2]}. \quad (\text{A9})$$

For $G_0 = 0.007$ the exponential factor gives a multiple 10^{125} , hence zero sound propagates without attenuation across the dense stellar crust for any imaginable values of frequency and temperature at which the Fermi liquid theory is still valid ($\hbar\omega, k_B T \ll E_F$). However, close to the stellar surface the electron gas becomes non relativistic. In this region the parameter G_0 depends on the density $G_0 \approx e^2 k_F / E_F = 0.65 / a_B n^{1/3}$, where $a_B = \hbar^2 / m_e e^2 = 0.53 \text{ \AA}$ is the Bohr radius, and could be of the order of 1 near the surface. However, in the surface region the effect of magnetic field becomes substantial and prevents the wave damping. We discuss this in another section.

B. Equations of magnetic hydrodynamics for electron motion

In this section we consider equations which describe wave propagation across the stellar crust. Typical temperature in the crust of middle-aged NSs is less than the melting temperature (Potekhin et al. 1997). As a result the matter forms a Coulomb crystal. One should note that zero-point ion vibrations do not destroy the lattice made of heavy nuclei. The amplitude of zero-point vibrations is commonly much smaller than typical inter-ion spacing. With increasing density the relative amplitude becomes larger, so that the vibrations can prevent crystallization at high ρ . The crystallization is completely suppressed in the so called quantum liquids, which exist at $\rho_6 > 0.006 A^4 Z^6$ (Jones & Ceperley 1996). The suppression is pronounced for light nuclei, however it does not occur in the lattice composed from heavy elements which is likely the case in the stellar crust. E.g., for iron lattice ($A = 56, Z = 26$) the density at which zero-point vibrations melt the lattice is $\rho > 2 \times 10^{19} \text{ g/cm}^3$. This value is much larger than the density at the crust bottom (10^{14} g/cm^3) and, therefore, vibrations do not destroy the lattice in the crust.

In our model we assume that crust consists of nuclei which form a lattice and a gas of free electrons. Free neutrons appear in the inner crust. Frequencies of radiation we are interested in are much larger than frequency of electron-electron and electron-phonon collisions. Hence, the electron gas can be treated as collisionless. As we have seen in the Appendix A, in collisionless regime zero sound is a possible collective excitation in electron liquid without magnetic field. It is known that in a strong magnetic field, such that $u_A \gg v_F$ (here $u_A = H / \sqrt{4\pi\rho_e}$ is the Alfvén velocity for electrons, ρ_e is the electron density), the collective excitations of electrons in compensated metals reduce to magnetoplasma waves (Buchsbaum & Galt 1961; Kaner & Skobov 1963). Their nature is similar to magnetosonic and Alfvén waves in magnetic hydrodynamics. The dispersion relations of magnetoplasma waves can be obtained from the dielectric permittivity of collisionless plasma in a magnetic field. Indeed, if only electrons contribute to the permittivity then (Lifshitz & Pitaevskii 1979)

$$\varepsilon_{\perp} = 1 - \frac{\omega_{pe}^2}{\omega^2 - \omega_{He}^2}, \quad (\text{B1})$$

where $\omega_{pe} = \sqrt{4\pi e^2 n_e / m_e}$ is the electron plasma frequency and $\omega_{He} = eH / m_e c$ is the electron cyclotron frequency. For this ε_{\perp} the dispersion equation for electromagnetic waves at $\omega \ll \omega_{He}$ has two solutions $\omega = k u_A / \sqrt{1 + u_A^2 / c^2}$ and $\omega = k u_A \cos \vartheta / \sqrt{1 + u_A^2 / c^2}$ describing the fast magnetosonic and Alfvén waves respectively (here ϑ is the angle between the wavevector \mathbf{k} and \mathbf{H}).

In magnetic hydrodynamics the fast magnetosonic wave reduces to usual sound in the limit of small magnetic field (when $u_A \ll u_s$). Here we demonstrate that such situation remains also valid in the collisionless regime with zero sound playing the role of usual sound. For this purpose it is convenient to use a definition of elementary excitations in electron liquid in terms of electron-hole pairs. In such picture the excitation with $p > p_F$ (particle) has the energy $\varepsilon = v_F(p - p_F)$, while at $p < p_F$ (hole) the energy is $\varepsilon = v_F(p_F - p)$, where p_F is the Fermi momentum. In such definition the excitation energy is positive and gives the energy excess above the ground state. Elementary excitations appear in pairs so that the total number of particles is always equal to the total number of holes. The dynamics of excitations is described by the collisionless kinetic equation for the quasiparticle distribution function $n(t, \mathbf{r}, \mathbf{p})$:

$$\frac{\partial n}{\partial t} + \mathbf{v} \frac{\partial n}{\partial \mathbf{r}} - \frac{\partial n}{\partial \mathbf{p}} \int f(\mathbf{p}, \mathbf{p}') \frac{\partial n(\mathbf{p}')}{\partial \mathbf{r}} \frac{d^3 p'}{(2\pi\hbar)^3} + e \left[\mathbf{E} + \frac{1}{c} (\mathbf{v} \times \mathbf{H}) \right] \frac{\partial n}{\partial \mathbf{p}} = 0, \quad (\text{B2})$$

where $\mathbf{v} = \partial \varepsilon / \partial \mathbf{p}$ and \mathbf{p} are the quasiparticle velocity and momentum. The quasiparticle charge and the mass are given by $e = |e| \text{sign}(p_F - p)$ and $m = m_e \text{sign}(p - p_F)$ respectively. The function $f(\mathbf{p}, \mathbf{p}')$ describes interactions between quasiparticles and determines the velocity of zero sound. For simplicity we assume that $f(\mathbf{p}, \mathbf{p}')$ does not contain a dependence on the quasiparticle spins. The equilibrium distribution function is $n_0 = 1 / [\exp(\varepsilon / k_B T) + 1]$, so that the equilibrium quasiparticle number depends on temperature.

Let us first consider the case of zero external magnetic field. In general, the particle-particle interaction differs from the interaction between a particle and a hole. As a result, it is convenient to treat our system as composed of two components. Then dynamics of the particle (n_1) and the hole (n_2) distribution functions is described by the following equations

$$\frac{\partial n_1}{\partial t} + \mathbf{v} \frac{\partial n_1}{\partial \mathbf{r}} - \frac{\partial n_1}{\partial \mathbf{p}} \int \left[f_{11}(\mathbf{p}, \mathbf{p}') \frac{\partial n_1(\mathbf{p}')}{\partial \mathbf{r}} + f_{12}(\mathbf{p}, \mathbf{p}') \frac{\partial n_2(\mathbf{p}')}{\partial \mathbf{r}} \right] \frac{d^3 p'}{(2\pi\hbar)^3} - |e| \mathbf{E} \frac{\partial n_1}{\partial \mathbf{p}} = 0, \quad (\text{B3})$$

$$\frac{\partial n_2}{\partial t} + \mathbf{v} \frac{\partial n_2}{\partial \mathbf{r}} - \frac{\partial n_2}{\partial \mathbf{p}} \int \left[f_{22}(\mathbf{p}, \mathbf{p}') \frac{\partial n_2(\mathbf{p}')}{\partial \mathbf{r}} + f_{21}(\mathbf{p}, \mathbf{p}') \frac{\partial n_1(\mathbf{p}')}{\partial \mathbf{r}} \right] \frac{d^3 p'}{(2\pi\hbar)^3} + |e| \mathbf{E} \frac{\partial n_2}{\partial \mathbf{p}} = 0. \quad (\text{B4})$$

One can seek a solution of these equations in the form $n_\alpha = n_{0\alpha} + \delta n_\alpha$, where $\delta n_\alpha = (\partial n_{0\alpha} / \partial \varepsilon) \nu_\alpha(\mathbf{p}) \exp[i(\mathbf{k}\mathbf{r} - \omega t)]$ is a small correction, $\alpha = 1, 2$. Here the function ν_α depends only on the direction of \mathbf{p} since $\partial n_0 / \partial \varepsilon$ is nonnegligible only when $p \approx p_F$. For simplicity we assume $f_{\alpha\beta}(\mathbf{p}, \mathbf{p}')$ to be constant. Then using $\partial n_0 / \partial \mathbf{p} = \mathbf{v} \partial n_0 / \partial \varepsilon$ and $d^3 p = p_F^2 d\Omega dp$ we obtain equations for ν_α

$$(\omega - \mathbf{k}\mathbf{v}) \nu_1(\mathbf{p}) - \mathbf{k}\mathbf{v} \int [F_{11} \nu_1(\mathbf{p}') + F_{12} \nu_2(\mathbf{p}')] \frac{d\Omega'}{4\pi} - i|e| \mathbf{E}\mathbf{v} = 0, \quad (\text{B5})$$

$$(\omega - \mathbf{k}\mathbf{v}) \nu_2(\mathbf{p}) - \mathbf{k}\mathbf{v} \int [F_{22} \nu_2(\mathbf{p}') + F_{21} \nu_1(\mathbf{p}')] \frac{d\Omega'}{4\pi} + i|e| \mathbf{E}\mathbf{v} = 0, \quad (\text{B6})$$

where $F_{\alpha\beta} = -4\pi p_F^2 \int f_{\alpha\beta} (\partial n_{0\beta} / \partial \varepsilon) dp / (2\pi\hbar)^3$ are dimensionless Landau parameters and $d\Omega'$ means integration over directions of \mathbf{p}' . Eqs. (B5), (B6) have to be solved simultaneously with the Maxwell equations for the electric field \mathbf{E} . However, as we have mentioned in Appendix A, in the zero sound regime the electric field of quasiparticles is screened by the rest part of electrons which fill the Fermi sphere and, hence, in Eqs. (B5), (B6) one can put $\mathbf{E} = \mathbf{0}$. The screening effect is included into Landau parameters $F_{\alpha\beta}$. One can consider the quasiparticles as moving in a medium with a very large dielectric constant $\varepsilon(\omega, \mathbf{k})$, then the Maxwell equation $\text{div}(\varepsilon \mathbf{E}) = 4\pi\rho$ results in $\mathbf{E} \cdot \mathbf{k} = 0$ which justifies the omitting \mathbf{E} . In our case of the two component particle-hole system $F_{11} = F_{22}$, $F_{12} = F_{21}$. Under such conditions Eqs. (B5), (B6) have the

following solutions describing longitudinal zero sound

$$\nu_1 = \frac{C \cos \theta}{s - \cos \theta}, \quad \nu_2 = \pm \frac{C \cos \theta}{s + \cos \theta}, \quad (\text{B7})$$

where $s = \omega/kv_F = u_s/v_F$ and θ is the angle between the wavevector \mathbf{k} and \mathbf{p} . The equation for s formally coincides with the expression obtained by Landau for a neutral Fermi liquid

$$\frac{s}{2} \ln \left(\frac{s+1}{s-1} \right) - 1 = \frac{1}{F_{11} \mp F_{12}} \quad (\text{B8})$$

in which the Fermi liquid interaction parameter $F = F_{11} \mp F_{12}$ (Dunin & Fetisov 1972). For the solution with the upper sign the particles and holes move with the same average velocity and the total current is equal to zero. Such solution also exists if there is no screening since the particle-hole motion does not produce electric field. Unscreened Coulomb interaction between particles is repulsive, that is $F_{11} > 0$, while particle-hole interaction is attractive $F_{12} < 0$. This suggests that $F = F_{11} - F_{12} > 0$ and, hence, the zero sound branch always exists in the system (not subject to Landau damping). For the solution with the lower sign the particles and holes move in opposite direction producing quasiparticle current and density oscillation. Such solution is allowed only when there is screening of the electric field.

Now let us discuss the effect of magnetic field. Here it is convenient to consider each of the components separately. For definiteness we derive equations of magnetic hydrodynamics in terms of (quasi)particle motion and use Eq. (B3) with the additional magnetic term. The average quasiparticle concentration n_q , the quasiparticle current density \mathbf{j}_q and the average velocity \mathbf{V}_q are given by

$$n_q = \int n_1 d^3p, \quad \mathbf{j}_q = \int e\mathbf{v}n_1 d^3p, \quad \mathbf{V}_q = \frac{\int \mathbf{v}n_1 d^3p}{\int n_1 d^3p}. \quad (\text{B9})$$

Integrating Eq. (B3) over d^3p we obtain the continuity equation

$$\frac{\partial n_q}{\partial t} + \nabla(n_q \mathbf{V}_q) = 0. \quad (\text{B10})$$

To derive an equation of momentum conservation in collisionless regime one should make an assumption about deformation in the distribution function. The assumption is necessary only when we integrate the term $\mathbf{v} \partial n_1 / \partial \mathbf{r}$ in the kinetic equation. Such a term is nonnegligible as compared to the magnetic field contribution only in the zero sound regime. Hence, without loss of generality one can assume that perturbation in the distribution function is similar to those for the longitudinal zero sound. Deviation of the sound speed u_s from v_F is determined by interactions between electrons f . However, at large densities the interaction energy is small compared with the electron kinetic energy and, therefore, $u_s \approx v_F$, that is $s - 1 \ll 1$. Under such condition, according to Eq. (B7), the deviation of the distribution function δn_1 from its equilibrium shape is extremely anisotropic. As a result, one may assume that δn_1 is nonzero only in a small vicinity of the direction given by the vector $\partial n_1 / \partial \mathbf{r}$. Also one can omit the small terms with f describing interactions and take n_0 instead of n_1 in the term with the electric field \mathbf{E} . Further, we assume that $\omega \ll \omega_{He}$. Such assumption makes possible to omit the term with electric field in the kinetic equation. The point is that the magnetic field \mathbf{H} does not allow the electron to move in a direction perpendicular to \mathbf{H} and change its average momentum in this direction under the influence of \mathbf{E} . So, if we are interested in the electron motion on a time scale larger than the Larmor period (that is $\omega \ll \omega_{He}$) only component of \mathbf{E} along \mathbf{H} can contribute to the change in electron momentum. Formally this follows from an equality $\mathbf{E}(\partial n_0 / \partial \mathbf{p}) = \mathbf{E}\mathbf{v}(\partial n_0 / \partial \varepsilon)$ in which the electron velocity $\mathbf{v} = \partial \varepsilon / \partial \mathbf{p}$ after averaging over fast Larmor precession has nonzero component

only along \mathbf{H} . Therefore, in the kinetic equation one can substitute \mathbf{E} by its component along the magnetic field. For simplicity of derivations we omit completely the term with the electric field bearing in mind that solutions of final equations are valid when they possess a property $\mathbf{E} \cdot \mathbf{H} = 0$, which is the case for magnetosonic waves we are focusing on. Then multiplying Eq. (B3) on \mathbf{v} and integrating over d^3p we obtain the following analog of Euler's equation in collisionless regime

$$\frac{\partial(n_q \mathbf{V}_q)}{\partial t} + v_F^2 \nabla n_q - \frac{1}{cm_e} (\mathbf{j}_q \times \mathbf{H}) = 0. \quad (\text{B11})$$

Further we note that if quasiparticles move with an average velocity \mathbf{V}_q then such motion induces an electric field $\mathbf{E} = -(1/c)(\mathbf{V}_q \times \mathbf{H})$. The reason is the large electric conductivity σ of the system which requires the total force exerting on quasiparticles to be equal to zero. The induced electric field also acts on the rest part of electrons filling the Fermi sphere. As a result, these electrons must move with some average velocity \mathbf{V} to insure the equality $\mathbf{E} + (1/c)(\mathbf{V} \times \mathbf{H}) \approx 0$. We obtain that magnetic field couples the motion of quasiparticles and electrons inside the Fermi surface. Equation $(\mathbf{V}_q \times \mathbf{H}) \approx (\mathbf{V} \times \mathbf{H})$ suggests that the quasiparticle current \mathbf{j}_q is related to the entire current density \mathbf{j} by $(\mathbf{j}_q \times \mathbf{H}) = (n_q/n_e)(\mathbf{j} \times \mathbf{H})$, where n_e is the total concentration of electrons in the system.

Further, using Maxwell's equations $\text{curl} \mathbf{H} = 4\pi \mathbf{j}/c + (1/c)\partial \mathbf{E}/\partial t$, $\text{curl} \mathbf{E} = -(1/c)\partial \mathbf{H}/\partial t$ and $\mathbf{j} = \sigma[\mathbf{E} + (1/c)(\mathbf{V}_q \times \mathbf{H})]$ we obtain equations of magnetic hydrodynamics for quasiparticle motion (in linearized form):

$$\frac{\partial \mathbf{H}}{\partial t} = \text{curl}(\mathbf{V}_q \times \mathbf{H}) + \frac{c^2}{4\pi\sigma} \left(\Delta \mathbf{H} - \frac{1}{c^2} \frac{\partial^2 \mathbf{H}}{\partial t^2} \right), \quad (\text{B12})$$

$$\frac{\partial \mathbf{V}_q}{\partial t} = -\frac{v_F^2}{n_q} \nabla n_q - \frac{1}{4\pi\rho_e} (\mathbf{H} \times \text{curl} \mathbf{H}) - \frac{1}{4\pi c^2 \rho_e} \left(\mathbf{H} \times \left(\frac{\partial \mathbf{V}_q}{\partial t} \times \mathbf{H} \right) \right) + \frac{|e|}{4\pi c m_e \sigma} \left(\frac{\partial \mathbf{V}_q}{\partial t} \times \mathbf{H} \right), \quad (\text{B13})$$

where $\rho_e = m_e n_e$ is the total density of electrons. The last term in Eq. (B12) describes attenuation of magnetosonic waves due to finite conductivity σ . It is interesting to note, that for waves propagating with velocity close to the speed of light (which is the case for ultrarelativistic electrons in the stellar crust) the dissipative term goes to zero and attenuation of magnetosonic waves is substantially suppressed.

In the limit of large conductivity ($\sigma \rightarrow \infty$) Eqs. (B10), (B12), (B13) reduce to usual equations of nondissipative magnetic hydrodynamics in which speed of sound is equal to the Fermi velocity and quasiparticle density undergoes oscillations instead of the total density of electrons:

$$\frac{\partial \mathbf{h}}{\partial t} = \text{curl}(\mathbf{V}_q \times \mathbf{H}), \quad (\text{B14})$$

$$\frac{\partial n'_q}{\partial t} + n_q \text{div} \mathbf{V}_q = 0, \quad (\text{B15})$$

$$\frac{\partial \mathbf{V}_q}{\partial t} = -\frac{v_F^2}{n_q} \nabla n'_q - \frac{1}{4\pi\rho_e} (\mathbf{H} \times \text{curl} \mathbf{h}) - \frac{1}{4\pi c^2 \rho_e} \left(\mathbf{H} \times \left(\frac{\partial \mathbf{V}_q}{\partial t} \times \mathbf{H} \right) \right), \quad (\text{B16})$$

where \mathbf{H} , n_q are equilibrium values of the magnetic field and quasiparticle density, while \mathbf{h} , n'_q are small perturbations. The last term in Eq. (B16) appears due to the displacement current in Maxwell's equations. Similar derivations can be done for the hole component, they result in the same equations (B14)-(B16) with n_h , \mathbf{V}_h instead of n_q , \mathbf{V}_q . Hence, one can seek a solution describing motion of one of the components independently, the equations of motion of the other component will be automatically satisfied, e.g., by taking $n_h = n_q$ and $\mathbf{V}_h = \mathbf{V}_q$.

Let us now derive an equation for propagation of magnetosonic waves. Taking div from both sides of Eq. (B16), using Eqs. (B14), (B15) and identities

$$\begin{aligned} \operatorname{div}(\mathbf{H} \times \operatorname{curl} \mathbf{h}) &= \operatorname{curl} \mathbf{h} \cdot \operatorname{curl} \mathbf{H} - \mathbf{H} \cdot \operatorname{curl}(\operatorname{curl} \mathbf{h}) \approx \mathbf{H} \cdot \Delta \mathbf{h}, \\ \operatorname{div} \left(\mathbf{H} \times \left(\frac{\partial \mathbf{V}_q}{\partial t} \times \mathbf{H} \right) \right) &= -\mathbf{H} \cdot \operatorname{curl} \left(\frac{\partial \mathbf{V}_q}{\partial t} \times \mathbf{H} \right) = -\mathbf{H} \cdot \frac{\partial^2 \mathbf{h}}{\partial t^2}, \end{aligned}$$

we obtain

$$\frac{\partial^2 n'_q}{\partial t^2} - v_F^2 \Delta n'_q - \frac{n_q}{4\pi\rho_e} \mathbf{H} \cdot \Delta \mathbf{h} + \frac{n_q}{4\pi c^2 \rho_e} \mathbf{H} \cdot \frac{\partial^2 \mathbf{h}}{\partial t^2} = 0. \quad (\text{B17})$$

The magnetic field \mathbf{H} creates the space anisotropy in our problem. It is convenient to decompose \mathbf{h} and \mathbf{V}_q into longitudinal (parallel to \mathbf{H}) and transverse (perpendicular to \mathbf{H}) components:

$$\mathbf{h} = \mathbf{h}_{\parallel} + \mathbf{h}_{\perp}, \quad \mathbf{V}_q = \mathbf{V}_{\parallel} + \mathbf{V}_{\perp}.$$

Then from Eqs. (B14), (B16) we find

$$\frac{\partial h_{\parallel}}{\partial t} = -H \operatorname{div} \mathbf{V}_{\perp}, \quad (\text{B18})$$

$$\frac{\partial \mathbf{h}_{\perp}}{\partial t} = (\mathbf{H} \cdot \nabla_{\parallel}) \mathbf{V}_{\perp}, \quad (\text{B19})$$

$$\frac{\partial \mathbf{V}_{\parallel}}{\partial t} = -\frac{v_F^2}{n_q} \nabla_{\parallel} n'_q. \quad (\text{B20})$$

Using Eqs. (B15), (B18) and (B20), we obtain

$$\frac{\partial^2 n'_q}{\partial t^2} - v_F^2 \Delta_{\parallel} n'_q - \frac{n_q}{H} \frac{\partial^2 h_{\parallel}}{\partial t^2} = 0, \quad (\text{B21})$$

where $\Delta_{\parallel} \equiv \nabla_{\parallel}^2$. Finally, Eqs. (B17), (B21) result in the following equation for wave propagation

$$\left(1 + \frac{u_A^2}{c^2} \right) \frac{\partial^4 n'_q}{\partial t^4} - \left((v_F^2 + u_A^2) \Delta + \frac{v_F^2 u_A^2}{c^2} \Delta_{\parallel} \right) \frac{\partial^2 n'_q}{\partial t^2} + v_F^2 u_A^2 \Delta_{\parallel} \Delta n'_q = 0, \quad (\text{B22})$$

where $u_A = H/\sqrt{4\pi\rho_e}$ is the Alfvén velocity determined by the total electron density.

Let us consider a plane magnetosonic wave with the wavevector \mathbf{k} : $n'_q \propto \exp(i\omega t - i\mathbf{k}\mathbf{r})$. Then Eq. (B22) gives the following expression for the speed of fast magnetosonic wave

$$u^2 = \left(v_F^2 + u_A^2 + \frac{v_F^2 u_A^2 \cos^2 \vartheta}{c^2} + \sqrt{\left[v_F^2 + u_A^2 + \frac{v_F^2 u_A^2 \cos^2 \vartheta}{c^2} \right]^2 - 4 \left(1 + \frac{u_A^2}{c^2} \right) v_F^2 u_A^2 \cos^2 \vartheta} \right) / 2(1 + u_A^2/c^2), \quad (\text{B23})$$

where ϑ is the angle between the wavevector \mathbf{k} and the magnetic field \mathbf{H} . Near the crust bottom $u_A \ll v_F$ and $u \approx v_F$ (the wave reduces to zero sound) while at the star surface $u_A \gg v_F$ and $u \approx u_A/\sqrt{1 + u_A^2/c^2}$ (magnetoplasma wave). We conclude that everywhere inside the stellar crust the speed of fast magnetosonic wave is approximately equal to the speed of light and, therefore, trajectories of rays are approximately straight lines.

C. Propagation of electromagnetic waves across the stellar atmosphere

In this section we discuss conditions at which electromagnetic radiation produced by vortices propagates across the stellar atmosphere without attenuation. The NS atmosphere is a thin plasma layer. Due to huge gravitational field $g \sim 10^{14} - 10^{15} \text{cm/s}^2$ at the surface, the NS atmospheres are extremely compressed. The scale height, $\sim Zk_B T_s / Mg$ (M and Z is the mass and charge of ions, T_s is the surface temperature), lies in the range $0.1 - 100 \text{cm}$ (Pavlov et al. 1995). Typical densities of the NS atmospheres are $0.1 - 10 \text{g/cm}^3$. The density grows with increasing g and decreases with increasing the atmosphere temperature. To be specific we assume ionized hydrogen atmosphere ($Z = 1$, $m = m_e$, $M = m_p$). A strong magnetic field of the order of $10^{12} - 10^{13} \text{Gs}$ can exist near the star magnetic poles. In such magnetic field the cyclotron frequency of electrons is (we take in numerical estimates $H = 4 \times 10^{12} \text{Gs}$)

$$\omega_{He} = \frac{|e|H}{mc} = 1.1 \times 10^{19} \text{s}^{-1}, \quad (\text{C1})$$

while the ion cyclotron frequency

$$\omega_{Hi} = \frac{|e|H}{Mc} = 6 \times 10^{15} \text{s}^{-1}, \quad (\text{C2})$$

here e is the electron charge. The strong magnetic field drastically distort the structure of atoms and increases the binding energies of electrons in atoms. For instance, the field 10^{12}Gs amplifies the binding energy of hydrogen atom to $\sim 150 \text{eV} \approx 1.7 \times 10^6 \text{K}$. For lower temperatures the magnetized atmospheres become partly ionized. In this section we assume that the atmosphere temperature is greater than 10^6K so that the magnetoactive plasma is highly ionized with $n_e = n_i = n$ (n_e and n_i are electron and ion concentrations). In numerical estimates we take $T_s = 2 \times 10^6 \text{K}$.

An effective collision frequency of particles characterizes the plasma. For parameters of the stellar atmosphere $\omega_{He} \gg k_B T_s / \hbar \approx 4 \times 10^{16} \text{Hz}$ that is thermal energy is much less then the spacing between Landau levels of electron in magnetic field. Therefore, collisions of an electron with other particles are substantially suppressed because the electron motion is effectively one dimensional (only momentum along the magnetic field can be changed during the collision). Contrary to electrons, spacing between Landau levels of ions is small in comparison with the temperature ($\hbar \omega_{Hi} \ll k_B T_s$) and, as a result, the ion-ion collisions are dominant. The effective ion-ion collision frequency can be estimated as (Ginzburg 1970)

$$\nu_{\text{eff}} \approx \frac{\pi e^4}{\sqrt{2}(k_B T_s)^2} \bar{v}_i n_i \ln \left(\frac{k_B T_s}{e^2 n_i^{1/3}} \right) = \frac{3.9 n_i}{T_s^{3/2}} \sqrt{\frac{m}{M}} \ln \left(\frac{220 T_s}{n_i^{1/3}} \right), \quad (\text{C3})$$

here \bar{v}_i is the average ion velocity. Magnetic field does not affect the nature of collisions provided $r_H \gg r_D$, where $r_H = \bar{v}_i / \omega_{Hi}$ is the radius of curvature of a particle in the field and $r_D \sim \bar{v}_i / \omega_{pi}$ is the Debye radius. From this we arrive at condition $\omega_{pi} \gg \omega_{Hi}$. If this condition is not satisfied (as in our problem), this fact, however, affects only the logarithmic factor in (C3) and Eq. (C3) still can be used for approximate estimation of the collision frequency. For $n_i = 10^{24} \text{cm}^{-3}$, $T_s = 2 \times 10^6 \text{K}$ we obtain that ν_{eff} lies in the infrared band: $\nu_{\text{eff}} \approx 4.7 \times 10^{13} \text{Hz}$. For colder NSs the atmosphere temperature is less than $\sim 10^6 \text{K}$, plasma is weakly ionized and ion-atom collisions become dominant.

For $n = 10^{24} \text{cm}^{-3}$ the plasma frequencies are

$$\omega_{pe} = \sqrt{\frac{4\pi e^2 n}{m}} = 9 \times 10^{15} \text{s}^{-1},$$

$$\omega_{pi} = \sqrt{\frac{4\pi e^2 n}{M}} = 2.1 \times 10^{14} \text{s}^{-1}.$$

We consider electromagnetic waves in plasma under the condition $\omega \gg \nu_{\text{eff}}$ (collisionless plasma) which suggests their small damping. The opposite limit $\omega \ll \nu_{\text{eff}}$ corresponds to magnetic hydrodynamics. We choose a coordinate system so that the z axis is oriented along the magnetic field \mathbf{H} . The dielectric permittivity tensor of a cold collisionless plasma in a magnetic field has the form (Lifshitz & Pitaevskii 1979)

$$\varepsilon_{xx} = \varepsilon_{yy} = \varepsilon_{\perp}, \quad \varepsilon_{zz} = \varepsilon_{\parallel}, \quad (\text{C4})$$

$$\varepsilon_{xy} = -\varepsilon_{yx} = i\eta, \quad \varepsilon_{xz} = \varepsilon_{yz} = 0, \quad (\text{C5})$$

$$\varepsilon_{\perp} = 1 - \frac{\omega_{pe}^2}{\omega^2 - \omega_{He}^2} - \frac{\omega_{pi}^2}{\omega^2 - \omega_{Hi}^2}, \quad (\text{C6})$$

$$\varepsilon_{\parallel} = 1 - \frac{\omega_{pe}^2 + \omega_{pi}^2}{\omega^2}, \quad (\text{C7})$$

$$\eta = \frac{\omega_{He}\omega_{pe}^2}{\omega(\omega^2 - \omega_{He}^2)} - \frac{\omega_{Hi}\omega_{pi}^2}{\omega(\omega^2 - \omega_{Hi}^2)}. \quad (\text{C8})$$

The dispersion equation for electromagnetic waves

$$\left| k^2 \delta_{\alpha\beta} - k_{\alpha} k_{\beta} - \frac{\omega^2}{c^2} \varepsilon_{\alpha\beta} \right| = 0 \quad (\text{C9})$$

has two solutions. One of them describes fast magnetosonic waves and for frequencies not too close to cyclotron frequencies ω_{Hi} , ω_{He} has the form

$$\omega = \frac{kc}{\sqrt{\varepsilon_{\perp}}}. \quad (\text{C10})$$

The other solution corresponds to Alfvén branch. General expression for the dispersion relation of this branch reduces to a simple form only in limiting cases. E. g., in the frequency range $\nu_{\text{eff}} \ll \omega \ll \omega_{Hi}, \omega_{pe}$ the dispersion equation for Alfvén waves is

$$\omega = \frac{c\omega_{pe}k \cos \vartheta}{\sqrt{\varepsilon_{\perp}} \sqrt{(kc \sin \vartheta)^2 + \omega_{pe}^2}}, \quad (\text{C11})$$

where ϑ is the angle between \mathbf{k} and \mathbf{H} .

Further we consider the fast magnetosonic branch only because this type of waves is generated by vortices. Ion-ion collisions produce damping of electromagnetic waves. To estimate parameters at which the atmosphere is transparent for fast magnetosonic waves one can use the following expression for the complex dielectric permittivity (Ginzburg 1970)

$$\varepsilon_{\perp} = 1 - \frac{\omega_{pe}^2}{\omega^2 - \omega_{He}^2} - \frac{\omega_{pi}^2(\omega + i\nu_{\text{eff}})}{\omega[(\omega + i\nu_{\text{eff}})^2 - \omega_{Hi}^2]} \approx 1 - \frac{\omega_{pe}^2}{\omega^2 - \omega_{He}^2} - \frac{\omega_{pi}^2}{\omega^2 - \omega_{Hi}^2} + \frac{i\nu_{\text{eff}}}{\omega} \frac{\omega_{pi}^2(\omega^2 + \omega_{Hi}^2)}{(\omega^2 - \omega_{Hi}^2)^2}. \quad (\text{C12})$$

At frequencies not too close to cyclotron frequencies the real part of the refractive index is $\text{Re}t \approx 1$, while the imaginary part is

$$\text{Im}t = \text{Im}\sqrt{\varepsilon_{\perp}} \approx \frac{\nu_{\text{eff}}}{2\omega} \frac{\omega_{pi}^2(\omega^2 + \omega_{Hi}^2)}{(\omega^2 - \omega_{Hi}^2)^2}. \quad (\text{C13})$$

If radiation propagates through the atmosphere along the z axis its amplitude decreases by a factor $\exp(-\omega \int \text{Im}t dz/c)$. In estimates we assume an isothermal atmosphere. Deviation of the atmosphere from an isothermal one

does not change the result substantially. Then concentration of particles changes with the height z as $n(z) = n_0 \exp(-Mgz/k_B T_s)$, where n_0 is the concentration at the atmosphere bottom ($z = 0$). The effective collision frequency $\nu_{\text{eff}} \propto n(z)$, and, therefore, $\text{Im}t \propto n^2$ also decreases with the height according to the exponential dependence. Using the criteria $\omega \int \text{Im}t dz/c \approx 1$ one can estimate the maximum density at the atmosphere bottom for which the atmosphere is still transparent for vortex radiation

$$n_0 \nu_{\text{eff}} \approx \frac{cgM^2}{\pi e^2 k_B T_s} \frac{(\omega^2 - \omega_{Hi}^2)^2}{(\omega^2 + \omega_{Hi}^2)}. \quad (\text{C14})$$

Comparing Eqs. (C14) and (C3), we finally obtain

$$n_0 \approx \frac{M^{1/4} g^{1/2} T_s^{1/4} H}{m^{1/4} \sqrt{3.9\pi \ln(220T_s/n^{1/3})} ck_B} \begin{cases} 1, & \omega \ll \omega_{Hi} \\ \omega/\omega_{Hi}, & \omega \gg \omega_{Hi} \end{cases}. \quad (\text{C15})$$

In the limit $\omega \ll \omega_{Hi}$ the maximum value of n_0 is independent of ω . If $g = 10^{15} \text{cm/s}^2$, $T_s = 2 \times 10^6 \text{K}$ and $H = 4 \times 10^{12} \text{Gs}$ we obtain $n_0 \approx 4.4 \times 10^{24} \text{cm}^{-3}$. In this limit Eq. (C15) approximately coincides with the photosphere density obtained from numerical calculations assuming free-free opacity (Lai et al. 1992): $n_{\text{phot}}(H) \approx 1.8 \cdot 10^{23} g^{1/2} T_s^{1/4} H_{12} = 4.8 \times 10^{24} \text{cm}^{-3}$. For $\omega > \omega_{Hi}$ the maximum value of n_0 becomes frequency dependent and increases with increasing ω . We conclude that if the particle concentration at the atmosphere bottom is less than $4 \times 10^{24} \text{cm}^{-3}$ (which is usually the case) the atmosphere is transparent for vortex radiation (apart from narrow regions near cyclotron frequencies).

REFERENCES

- Abel, W. R., Anderson, A. C. & Wheatley, J. C. 1966, *Phys. Rev. Lett.*, 17, 74
- Alpar, M. A., Langer, S. A. & Sauls, J. A. 1984, *ApJ*, 282, 533
- Ambegaokar, V., Halperin, B. I., Nelson, D. R., & Siggia, E. D. 1980, *Phys. Rev. B*, 21, 1806
- Amundsen, L. & Ostgaard, E. 1985a, *Nucl. Phys. Ser. A*, 437, 487
- Amundsen, L. & Ostgaard, E. 1985b, *Nucl. Phys. Ser. A*, 442, 163
- Arndt, R. A., Strakovsky, I. I. & Workman, R. L. 1994, *Phys. Rev. C*, 50, 2731
- Arndt, R. A., Oh, C. H., Strakovsky, I. I. & Workman, R. L. 1997, *Phys. Rev. C*, 56, 3005
- Arovas, D. P. & Freire, J. A. 1997, *Phys. Rev. B*, 55, 1068
- Baldo, M., Elgaroy, O., Engvik, L., Hjorth-Jensen, M. & Schulze, H. J. 1998, *Phys. Rev. C*, 58, 1921
- Baldo, M. & Grasso, A. 2001, *Phys. of Atomic Nuclei*, 64, 611
- Barenghi, C. F. 1996, *Phys. Rev. A*, 54, 5445
- Baym, G., Pethick, C., & Pines, D. 1969, *Nature*, 224, 673
- Becker, W. & Trümper, J. 1997, *A&A*, 326, 682
- Bezuglyi, E. V., Burma, N. G., Deineka, E. Yu., Fil', V. D. & Kaufmann, H. J. 1991, *J. Phys.: Condens. Matter* 3, 7867

- Bezuglyi, E. V., Boichuk, A. V., Burma, N. G. & Fil', V. D. 1995, *Fiz. Nizk. Temp.* 21, 633 [*Low Temp. Phys.* 21, 493 (1995)]
- Blandford, R. D., Applegate, J. H. & Hernquist, L. 1983, *MNRAS*, 204, 1025
- Buchsbaum, S. J. & Galt, J. K. 1961, *Phys. Fluids* 4, 1514
- Burma, N. G., Deineka, E. Yu. & Fil', V. D. 1989, *Pis'ma Zh. Eksp. Teor. Fiz.* 50, 18 [*JETP Lett.* 50, 20 (1989)]
- Corruccini, L. R., Clarke, J. S., Mermin, N. D. & Wilkins, J. W. 1969, *Phys. Rev.* 180, 225
- Cottam, J., Paerelsand, F. & Mendez, M. 2002, *Nature*, 420, 51
- Douchin, F. & Haensel, P. 2000, *Phys. Lett. B*, 485, 107
- Dunin, S. Z. & Fetisov, E. P. 1972, *Fiz. Tverd. Tela (Leningrad)* 14, 270 [*Sov. Phys. Solid State* 14, 221 (1972)]
- Elgaroy, O., Engvik, L., Hjorth-Jensen, M. & Esnes, E. 1996, *Nucl. Phys. A*, 604, 466
- Fischer, U. R. 1999, *Ann. Phys.*, 278, 62
- Ginzburg, V. L. 1970, *The propagation of electromagnetic waves in plasma*. Pergamon Press
- Golden, A., Shearer, A., Redfern, R. M., Beskin, G. M., Neizvestny, S. I., Neustroev, V. V., Plokhotnichenko, V. L. & Cullum, M. 2000, *A&A*, 363, 617
- Gottfried, K. & Pičman, L. 1960, *K. Dan. Vidensk. Selsk. Mat. Fys. Medd.* 32, no. 13
- Gor'kov, L. P. & Dzyaloshinskii, I. E. 1963, *Zh. Eksp. Teor. Fiz.*, 44, 1650 [*JETP* 17, 1111 (1963)]
- Halpern, J. P., Wang, F. Y.-H., 1997, *ApJ*, 477, 905
- Harding, A. K., Strickman, M. S., Gwinn, C., McCulloch, P. & Moffet, D. 1999, E-print astro-ph/9911263
- Harding, A. K., Strickman, M. S., Gwinn, C., Dodson, R., Moffet, D. & McCulloch, P. 2002, *ApJ*, 576, 376
- Hernquist, L., 1984, *ApJs*, 56, 325
- Hoffberg, M., Glassgold, A. E., Richardson, R. W. & Ruderman, M. 1970, *Phys. Rev. Lett.* 24, 775
- Jones, M. D. & Ceperley, D. M. 1996, *Phys. Rev. Lett.*, 76, 4572
- Kaner, E. A. & Skobov, V. G. 1963, *Zh. Eksp. Teor. Fiz.* 45, 610
- Keen, B. E., Matthews, P. W. & Wilks, J. 1965, *Proc. Roy. Soc. (London)*, A284, 125
- Kittel, C. 1968, *Introduction to Solid State Physics*, John Wiley & Sons, Inc., New York
- Koptsevich, A. B., Pavlov, G. G., Zharikov, S. V., Sokolov, V. V., Shibanov, Yu. A. & Kurt, V. G. 2001, *A&A*, 370, 1004
- Kurt, V. G., Sokolov, V. V., Zharikov, S. V., Pavlov, G. G., & Komberg, B. V. 1998, *A&A*, 333, 547
- Lai, D., Salpeter, E. E. & Shapiro, S. L. 1992, *In Isolated Pulsars*, Eds Van Riper, K. A., Epstein, R. & Ho, C. (Cambridge University Press), p. 164

- Lai, Dong, 2001, *Rev. Mod. Phys.*, 73, 629
- Landau, L. D. 1957, *Zh. Eksp. Teor. Fiz.*, 32, 59 [Sov. Phys. JETP 5, 101 (1957)]
- Landau, L. D. & Lifshits, E. M. 1960, *Electrodynamics of continuous media*, (Pergamon Press, London, 1960), Sec. 53, p. 224
- Lattimer, J. M., Pethick, C. J., Prakash, M. & Haensel, P. 1991, *Phys. Rev. Lett.*, 66, 2701
- Larson, M. B. & Link, B. 1999, *ApJ* 521, 271
- Lifshitz, E. M. & Pitaevskii, L. P. 1979, *Physics Kinetics*, (Nauka, Moscow)
- Lifshitz, E. M. & Pitaevskii, L. P. 1980, *Statistical Physics*, Part 2, 3rd edition (Pergamon, Oxford, 1980)
- Lundh, E. & Ao, P. 2000, *Phys. Rev. A*, 61, 063612
- Martin, C., Halpern, J. P. & Schiminovich, D. 1998, *ApJ*, 494, L211
- Mermin, N. D. 1967, *Phys. Rev.* 159, 161
- Mignani, R. P., Caraveo, P. A. & Bignami, G. F. 1998, *A&A*, 332, L37
- Nasuti, F. P., Mignani, R. P., Caraveo, P. A. & Bignami, G. F. 1997, *A&A*, 323, 839
- Nygaard, N., Bruun, G. M., Clark, C. W. & Feder, D. L. 2002, E-print cond-mat/0210526
- Ovchinnikov, Yu. N. & Sigal, I. M. 1998, *Nonlinearity*, 11, 1295
- Page, D. 1995, *ApJ*, 442, 273
- Pavlov, G. G., Shibano, Yu. A., Zavlin, V. E. & Meyer, R. D. 1995, *In The lives of the neutron stars*, Eds Alpar, M. A., Kiziloğlu, Ü. & van Paradijs, J. (Dordrecht: Kluwer), p. 71
- Pavlov, G. G., Welty, A. D. & Cordova, F. A. 1997, *ApJ*, 489, L75
- Pavlov, G. G., Zavlin, V. E., Sanwal, D., Burwitz, V., & Garmire, G. P. 2001, *ApJ*, 552, L129
- Pethick, C. J. 1992, *Rev. Mod. Phys.*, 64, 1133
- Pines, D. & Nozieres, P. 1989, *The theory of quantum liquids*, (Addison-Wesley Publishing Co., New York, NY, 1989), p. 281
- Potekhin, A. Y., Chabrier, G. & Yakovlev, D. G. 1997, *A&A*, 323, 415
- Potekhin, A. Y., & Yakovlev, D. G. 1996, *A&A*, 314, 341
- Van Riper, K. A. 1988, *ApJ*, 329, 339
- Van Riper, K. A., Link, B. & Epstein, R. I. 1995, *ApJ*, 448, 294
- Romani, R. W. 1987, *ApJ*, 313, 718
- Ruderman, M., Zhu, T. & Chen, K. 1998, *ApJ*, 492, 267
- Sauls, J. A. 1989, *in Timing Neutron Stars*, Eds H. Ögelman & E. van den Heuvel (Dordrecht: Kluwer), 457

- Sedrakyan, D. M. & Shakhbasyan, K. M. 1991, *Usp. Fiz. Nauk*, 161, 3 [*Sov. Phys. Usp.*, 34, 555 (1991)].
- Shearer, A., Redfern, R. M., Gorman, G., Butler, R., Golden, A., O’Kane, P., Beskin, G. M., Neizvestny, S. I., Neustroev, V. V., Plokhotnichenko, V. L. & Cullum, M. 1997, *ApJ*, 487, L181
- Shearer, A., Golden, A., Harfst, S., Butler, R., Redfern, R. M., O’Sullivan, C. M. M., Beskin, G. M., Neizvestny, S. I., Neustroev, V. V., Plokhotnichenko, V. L., Cullum, M. & Danks, A. 1998, *A&A*, 335, L21
- Shibanov, Y. A. & Yakovlev, D. G. 1996, *A&A*, 309, 171
- Silin, V. P. 1958, *Zh. Eksp. Teor. Fiz.*, 35, 1243 [*JETP* 8, 870 (1959)]
- Sjöberg, O. 1976, *Nucl. Phys.*, A265, 511
- Strickman, M. S., Harding, A. K. & deJager, O. C. 1999, E-print astro-ph/9904357
- Svidzinsky, A. A. & Fetter, A. L. 2000a, *Phys. Rev. A*, 62, 063617
- Svidzinsky, A. A. & Fetter, A. L. 2000b, *Phys. Rev. Lett.*, 84, 5919
- Thompson, C. & Duncan, R. C. 1993, *ApJ*, 408, 194
- Thorolfsson, A., Rögnvaldsson, Ö. E., Yngvason, J. & Gudmundsson, E. H. 1998, *ApJ*, 502, 847
- Tkachenko, V. K. 1965, *Zh. Eksp. Teor. Fiz.*, 49, 1875 [*Sov. Phys. JETP* 22, 1282 (1966)]; *Zh. Eksp. Teor. Fiz.*, 50, 1573 (1966) [*Sov. Phys. JETP* 23, 1049 (1966)]
- Urpin, V. A., Levshakov, S. A. & Yakovlev, D. G. 1986, *MNRAS*, 219, 703
- Wiebicke, H. -J. & Geppert, U. 1996, *A&A*, 309, 203
- Yakovlev, D. G., Levenfish, K. P. & Shibanov, Yu. A. 1999a, *Usp. Fiz. Nauk*, 169, 825 [*Physics - Uspekhi*, 42, 737 (1999)]
- Yakovlev, D. G., Kaminker, A. D. & Levenfish, K. P. 1999b, *A&A*, 343, 650
- Yakovlev, D. G., Kaminker, A. D., Gnedin, O. Y. & Haensel, P. 2001, *Phys. Rep.* 354, 1
- Zhuravlev, O. N., Muryshev, A. E. & Fedichev, P. O. 2001, *Phys. Rev. A*, 64, 053601

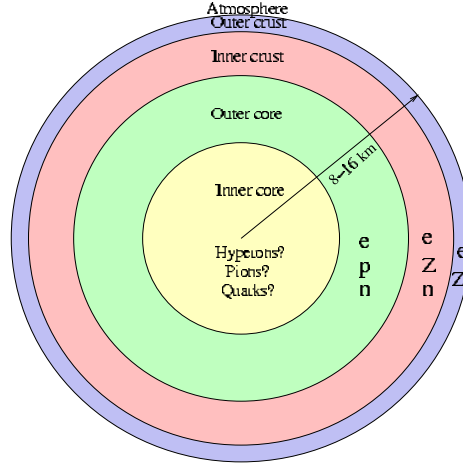


Fig. 1.— Schematic cross section of a dense neutron star. The star is subdivided into the atmosphere, the outer crust, the inner crust and superfluid outer and inner cores.

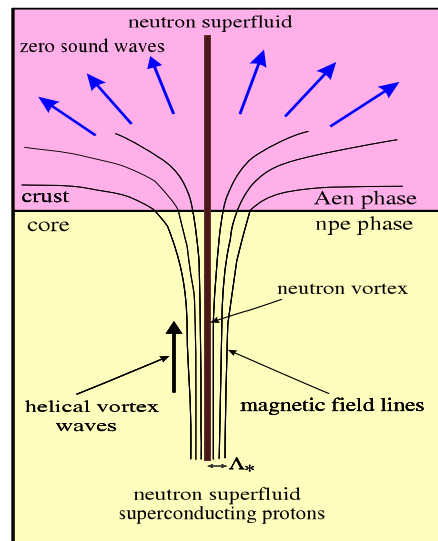


Fig. 2.— Generation of zero sound waves by vortices at the crust-core interface. Due to drag effect the helical vortex motion causes density oscillation of electrons in the stellar core. No sound is radiated inside the core because the wave length of sound is larger then the helix period. However, at the crust-core interface the density oscillation excites spherical sound waves that propagate across the stellar crust.

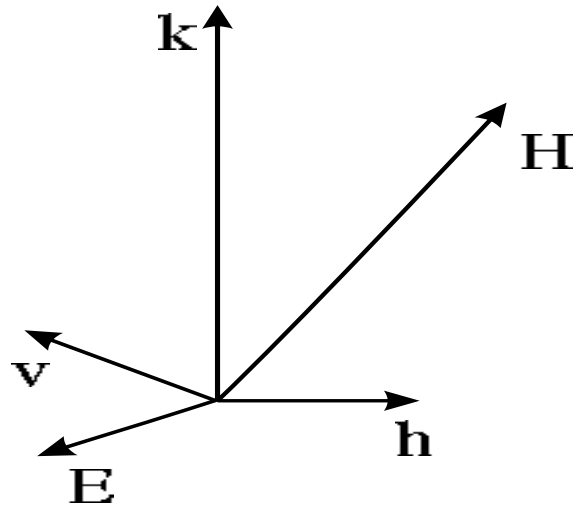


Fig. 3.— Oscillations of electric and magnetic fields in the fast magnetosonic wave in the limit $u_A \gg u_s$. Oscillating magnetic \mathbf{h} and electric fields \mathbf{E} are perpendicular to each other and the wavevector \mathbf{k} . The electron velocity \mathbf{V} lies in the kH plane and perpendicular to \mathbf{H} .

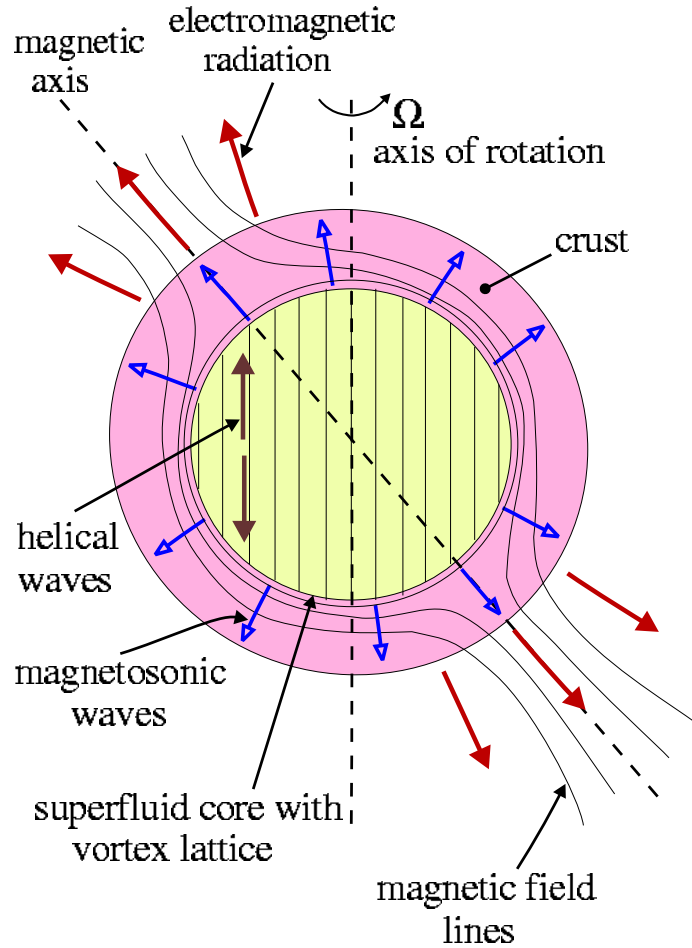


Fig. 4.— Mechanism of a neutron star radiation. Thermally excited helical waves of neutron vortices in the superfluid core produce magnetosonic waves in the stellar crust. Magnetosonic waves propagate across the crust and transform into electromagnetic radiation at the star surface. Mainly the radiation comes out from regions with strong magnetic field (near magnetic poles).

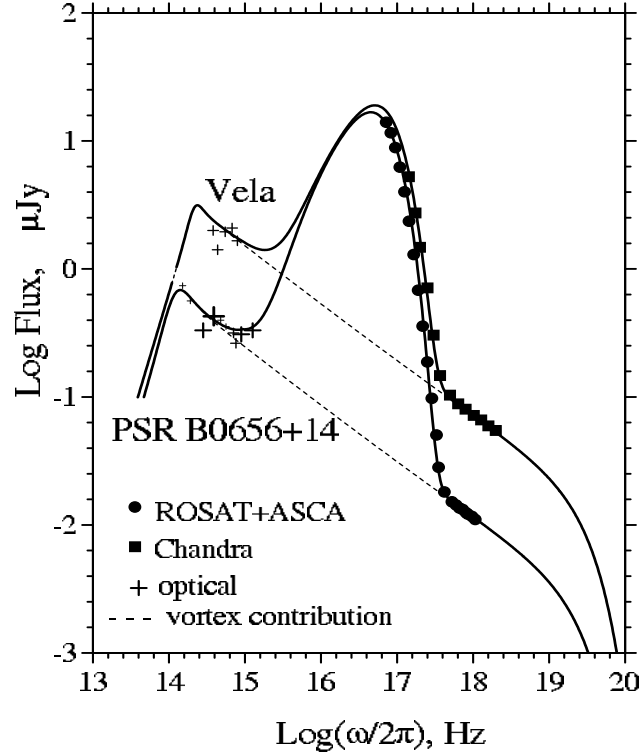


Fig. 5.— Broadband spectrum of PSR B0656+14 (Koptsevich et al. 2000) and the Vela pulsar (Pavlov et al. 2001, Nasuti et al. 1997). Solid line is the fit by the sum of the vortex and thermal components. Thermal radiation of the stellar surface dominates in the ultraviolet and soft X -ray bands, while the vortex contribution (dash line) prevails in infrared, optical and hard X -ray bands, where its spectrum has a slope $\alpha \approx -0.45$. In the far infrared band the spectrum of vortex radiation changes its behavior and follows Planck's formula with $P(\omega) \propto \omega^2$.

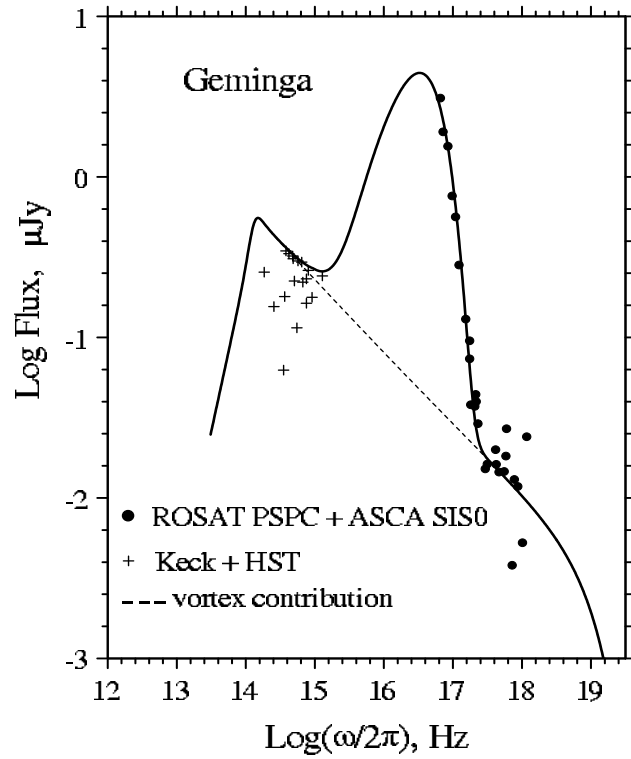


Fig. 6.— Broadband spectrum of the Geminga pulsar. Filled circles are data of ROSAT and ASCA (Halpern & Wang 1997), while crosses combine measurements of the Keck Observatory (Martin et al. 1998) and the Hubble Space Telescope (Mignani et al. 1998). Solid line is the fit by the sum of the vortex (dash line) and thermal contributions.

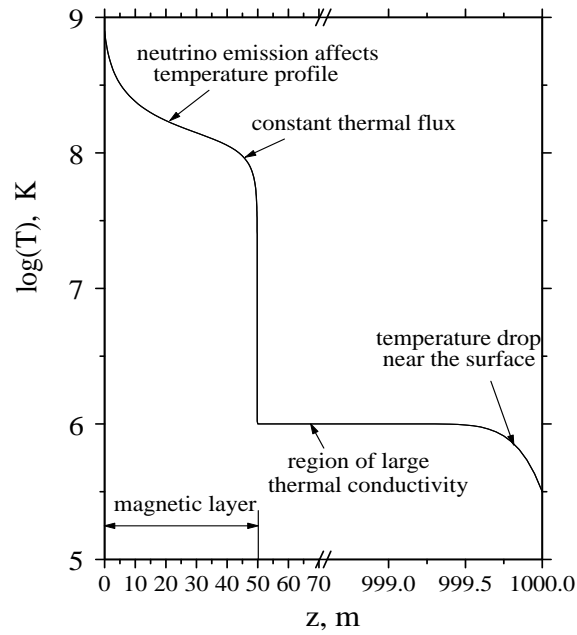


Fig. 7.— Temperature distribution in a neutron star crust for a model with magnetic isolating layer of width $d = 50\text{m}$. The main temperature drop occurs near the crust bottom where temperature decreases from $T = 8 \times 10^8\text{K}$ (at the core-crust interface, $z = 0$) to 10^6K . The rest part of the crust is approximately isothermal apart from a thin surface layer where temperature drops due to substantial decrease of thermoconductivity at low densities. Near the crust bottom the neutrino emissin results in energy losses and only a small fraction of the original heat flux reaches the stellar surface.